Chemical Characterization of the Degradation of Necromass from Four Ascomycete Fungi: Implications for Soil Organic Carbon Turnover and Storage

A Thesis
SUBMITTED TO THE FACULTY OF THE UNIVERSITY OF MINNESOTA
BY

Valerie Joan Bruner

IN PARTIAL FULFILLMENT OF THE REQUIREMENTS
FOR THE DEGREE OF
MASTER OF SCIENCE

Kathryn M Schreiner, Advisor

December, 2020

Acknowledgments

I would like to recognize and thank everyone that contributed to the content of this document and my time as a graduate student. First of all, my advisor, Dr. Kathryn Schreiner, has given of her time, experience, and (most importantly) patience for the quality of this document and the data. She has encouraged me to pursue my interest in this project and has driven me to always work a bit harder and to produce the best final product. I would also like to thank Julia Agnich for her technical help and expertise regarding all aspects of the laboratory work. Dr. Elizabeth Austin-Minor and Dr. Sergei Katsev have been instrumental as committee members in steering my project and focus in the correct direction. I would like to acknowledge Dr. Erin Sheets and her advice in writing the melanin isolation protocol and for lending the use of her laboratory space for this goal. I have to also acknowledge previous lab work on this project that was carried out at Northwestern University and the Chicago Botanic Garden by Dr. Schreiner, Dr. Louise Egerton-Warburton, Dr. Neal Blair, Benjamin Sedillo, and Allison Buiser. Dr. Egerton-Warburton has also been very helpful in reviving fungal tissue stored for years in the freezer.

Erik Hendrickson and Rachel Van Allen have also been instrumental in detecting and solving technical problems. Mojtaba Fakhraee has been helpful in advising on the figures found in this document. I would also like to thank Elijah Farley, R. Hunter Nickoloff, and Maeve Ryan for their help wrapping up the lab work for this project. The whole of my lab group has also been very supportive and accommodating, this includes Erik Bye, Gage Sachs and Rachel Van Allen. I would like to recognize immense support from the Large Lakes Observatory and the Chemistry and Biochemistry Department at UMD for administrative and monetary support.

I would finally like to acknowledge the personal support from my parents Peter and Michelle Bruner, and my sister Julie Bruner. My family has been so accommodating to my schedule as a graduate student.

ABSTRACT

Terrestrial soils store approximately twice as much carbon as is currently in the atmospheric CO_2 pool. Despite its importance in the global carbon cycle, much is still unknown about the source, turnover, and stability of the soil organic matter (SOM) pool. For example, fungi are known to play an important role in shaping the chemistry of SOM by degrading common biopolymers, and fungal biomass has been found to be a significant portion of living microbial SOM, dominating over bacteria in some soils by as much as 90%. And yet, despite growing evidence that microbial necromass, or dead microbial tissue, may be a larger contributor to SOM than previously thought, very little is known about the specific degradation patterns of fungal necromass, and subsequently its potential chemical contributions to long-lived SOM pools. This study addresses these knowledge gaps through a time-series analysis of the degradation patterns of fungal tissue from four different saprotrophic *Ascomyota* species in temperate restored prairie soils. Fungal tissue was buried in a temperate soil and harvested at intervals from 1 day to one month. After harvest, chemical analysis of the dried tissue by thermochemolysis pyrolysis-GCMS was used for relative quantitation of compounds derived from lipids, aromatics, carbohydrates, nitrogen-containing, and unspecified residues. The degradation of these specific molecules, bulk fungal tissue, and bulk C and N within the tissue, is modeled to (1) show that a small portion of fungal necromass persists in the environment even after the period of the experiment and could serve as a contributor to long-lived SOM, and (2) provide quantitative information on the contribution of fungal tissue to global SOM pools.

TABLE OF CONTENTS

LIST OF TABLES

LIST OF FIGURES

CHAPTER 1

1.1.Soil organic carbon

Worldwide, the top meter of terrestrial soils contains approximately 1500 Pg of carbon, twice that which exists as carbon dioxide in the atmosphere (Bernhardt and Schlesinger 2013). Through pathways of fixation, degradation, and respiration, soil organic matter (SOM) is linked to carbon dioxide and methane in the atmosphere, which is a major factor in anthropogenic global warming (IPCC 2013). Because the sources and chemistry of SOM has yet to be fully understood, the fate of this carbon pool is also uncertain under changing environmental conditions, including climate change. As such, it is important to characterize and understand the chemical reactions that control the fluxes and chemistry of the SOM pool to predict the future of this carbon pool in an environment increasingly affected by anthropogenic perturbations (Simpson and Simpson 2012).

SOM has a complicated chemical structure that cannot be explicitly defined. It is composed of many different molecules that make up living organisms, detritus, and individual chemical compounds (Simpson and Simpson 2012). These molecules that collectively form SOM are derived directly from living organic matter or created during organic matter degradation (Kögel-Knabner 2002). Compounds created during degradation can be the work of microbial attack or abiotic reactions (Schmidt et al. 2011; Sutton and Sposito 2005). Due to this heterogeneity, it is necessary to more precisely define SOM in terms of its sources, differing chemical makeup, and turnover such that bulk behavior can be better understood in a variety of environments.

Classically, it was thought that biomolecules derived from vegetation, mainly lignin, underwent extensive polymerization and rearrangement reactions to become large, highly aromatic compounds that accumulated in the soils as humic substances (Piccolo et al. 2002) and contributed to the bulk of SOM. Lignin and humic substances were operationally defined by extraction method and were found to have similar elemental makeup and molecular weights (Burges, Hurst, and Walkden 1964; Piccolo et al. 2002). Furthermore, these substances are thought to have similar chemical structures and degradation studies of plant lignin have resulted in similar-structured humic substances (Burges et al. 1964; Flaig 1964; Fogel and Cromack Jr. 1977). More recently, the view of soil composed of stable, lignin-derived OM has fallen out of favor as well as the harsh acid/base extraction techniques that this operationally defined paradigm relied on. Novel techniques that allow for the analysis of bulk soils without fractionation are changing the understanding of the structure and sources of SOM including the existence of microbial-derived SOM (Hedges et al. 2000; Lehmann and Kleber 2015).

A variety of factors are known to affect the turnover and stability of SOM. High OM C:N ratios are shown to correlate with slow degradation (Cotrufo, Ineson, and Roberts 1995; Koide and Malcolm 2009; Taylor, Parkinson, and Parsons 1989). The physical location of OM can also affect its stability as aggregate structures within the soil can make SOM physically inaccessible to microbes (Six et al. 2002). OM can also form intermolecular interactions with soil minerals that can decrease its degradability (Six et al. 2002). Finally, changing environmental conditions like increasing mean annual precipitation and increasing temperature correlate with increased OM degradation (Lloyd and Taylor 1994).

Saprotrophic fungi, which are fungi that actively degrade other biomass, are known to play important roles in SOM degradation. These fungi are the most important degraders of the three most common biopolymers: cellulose, lignin, and chitin; and are thus able to chemically alter OM that is delivered to the soils (Baldrian et al. 2010). With respect to lignin, fungi are the main degraders of this biopolymer and are able to fully degrade lignin (Brown and Chang 2014; Prewitt et al. 2014). When compared to plant litter and fine root inputs, Godbold (2006) found plant-associated fungi as the main mechanism through which carbon entered the SOM pool. In addition to their impacts on the chemistry of SOM, soil fungi also contribute to the physical structure of soils through soil aggregate formation. Aggregate formation by fungi occurs due to hyphal growth, wherein these aggregate structures can ensnare smaller particles, binding them into larger particles, which can physically occlude degraders (Tisdall and Oades 1982). Through this process, OM can be physically protected from degradation by microbes (Bossuyt et al. 2001; Hu et al. 1995; Tisdall and Oades 1982).

As described above, a portion of SOM is the living biomass of microbes and plant roots, of which fungal tissue is known to make up a large portion (Six et al. 2006). The total amount of microbes and the fungal contribution to this total is thought to be a function both of the chemical make-up and land use of the soil (Joergensen and Wichern 2008; Six et al. 2006). For instance, microbial activity is highest in clay and no-till cropland shows higher fungal contributions due to aggregate stabilization (Joergensen and Wichern 2008; Six et al. 2006). Because fungi actively form protective soil aggregates, in soils with high concentrations of fungi, fungal biomass, along with other forms of SOM, can also be protected from degradation (Six et al. 2006).

Furthermore, dead fungal tissue may also play an important role in stabilizing SOM. Fungal hyphae tissue has been found to resist degradation compared to bacterial biopolymers (Guggenberger et al. 1999), but there are conflicting hypotheses about why this might be. Relative degradation resistance may be due to the concentrations of melanin within the fungal tissue, as melanin molecules are hypothesized to be long lived within soils, and therefore would contribute to the long-lived SOM pool (Fernandez et al. 2019; Kögel-Knabner 2002; Linhares and Martin 1978; Ryan 2019; Ryan et al. 2020). In addition to the effects of melanin, degradation rates of fungi are also thought to depend on the nitrogen content of fungal tissue with increasing tissue loss resulting from nitrogen rich tissues (Fernandez et al. 2019; Koide and Malcolm 2009). Finally, increased species heterogeneity of degrading fungal necromass has also been found to correlate with higher degradation extent (Wilkinson, Alexander, and Johnson 2011). While all of these factors impact fungal tissue degradation to a certain extent, it is unclear how the importance of each factor varies with fungal species, specific environment, climate, and a variety of other factors, indicating more work is needed. Additionally, despite the importance of saprotrophic fungi in SOM degradation, cycling, and storage, studies to date have focused only on degradation of ectomycorrhizal fungal tissue, whereas saprotrophic fungi have been mostly overlooked in the literature (Drigo et al. 2012; Fernandez et al. 2019; Koide and Malcolm 2009; Ryan 2019; Ryan et al. 2020; Wilkinson et al. 2011).

1.2 Fungal biomolecules

Fungal cell walls have evolved with many different structures and chemistries (Figure 1.1). Not only does the cell wall structure vary across species, but it also varies

within species based on fungal structure and growth environment (Aguilar-Uscanga and Francois 2003; Francois 2007; Latgé 2007). Despite these differences, all cell wall structures include various carbohydrate polymers woven together and covalently bonded to other structures within the cell wall network to lend structural strength to the cell wall (Klis et al. 2002). The purpose of the cell wall is to protect the plasma membrane of the fungal cell, which is composed of phospholipids, proteins, and various sterols including the fungal-specific sterol, ergosterol (Nylund and Wallander 1992). Each of these compounds differ in physical stability and enzymatic catalytic breakdown pathways. In addition to differences in chemical makeup, different layering patterns within the cell walls of different fungi may selectively preserve some biomolecules over others.

Fungi use chitin as their main tissue structural support and the polymer forms 1-2% of the dry cell wall mass (Klis et al. 2002). The chitin polymer is composed of regular, repeating D *N*-acetylglucosamine monomers linked together in chains via β (1→4) ether bonds (Figure 1.2). In addition to the ether, hydroxyl, and carbonyl functional groups standard to polysaccharide structures, chitin is also characterized by an amide bond at the C2 position. The chitin polymer is fairly inelastic, due to electrostatic interactions that stabilize the stacking of these polysaccharide chains. Combining this inelasticity with its total polymer size, the chitin molecule may be able to physically discourage enzymatic degradation (Godbold et al. 2006; Langley and Hungate 2003; Treseder and Allen 2000).

Within soils there are a great variety of microbes that have chitinolytic properties (Gooday 1990), and there is high microbial assimilation of chitin and N-acetylglucosamine monomers when added to soil (Zeglin, Kluber, and Myrold 2012).

Although some have posited that chitin may resist degradation in the environment (Godbold et al. 2006; Langley and Hungate 2003; Treseder and Allen 2000), this has not seemed to be the case, at least in ectomycorrhizal species. Fernandez and Koide (2012) found increased chitin concentrations correlated to increased total decomposition of ectomycorrhizal fungal tissue. Furthermore, they observed a faster decay of chitin concentrations than total mass, indicating chitin is a more labile component of the fungal tissue. Supporting these findings, Drigo et al. (2012) found chitin-glucan complexes and a glucose derivative to decrease rapidly within the first week of ectomycorrhizal fungal tissue degradation, and then exhibit stable concentrations for the rest of a 28-day experiment.

In addition to chitin, glucans (Figure 1.3) and mannans (Figure 1.4) are also used for structural support in the fungal cell wall (Moore, Robson, and Trinci 2011). These sugars and others are thought to combine with chitin, proteins, and melanin to form a complex interlinking cell wall structure (Kollár et al. 1997; Moore, Robson, and Trinci 2011, Figure 1.1). Glucans are typically found as β(1-3) linked glucose chains up to 1500 residues long with occasional β(1-6) branching (Klis et al. 2002; Moore et al. 2011). In total, 50-65% of dry cell wall mass is glucans (Klis et al. 2002; Moore et al. 2011). Mannans are also an important contributor to cell wall mass, with mannans conjugated to proteins forming 35-40% of dry cell wall weight (Klis et al. 2002). Mannose monomers that are part of this structure form a α(1-6) link; however, this repeating sugar motif represents only ~5% of the mannoprotein structure (Ahrazem et al. 1997; Leal et al. 2010).

Microbial sugars are a stable portion of SOM in some soils (Glaser, Turrión, and Alef 2004; Roberts and Jones 2012; Tsai, Killham, and Cresser 1997). Peptidoglycan, composed of aminosugars and muramic acid, has concentrations in natural soils higher than in microbial biomass, suggesting a stabilization method within the soils themselves (Glaser et al. 2004). Amino sugars have been found less susceptible to uptake by microbes compared to free sugars in a degradation kinetics study (Roberts and Jones 2012) and a soil respiration study (Tsai et al. 1997). Amino sugar content of soil is significant as it represents 5% to 12% of soil organic nitrogen (Glaser and Amelung 2002; Stevenson 1983). This slower removal of nitrogen-containing sugar monomers could indicate a slower removal of chitin and mannoproteins from soils in comparison to glucan should be expected, in turn indicating a greater contribution from fungal carbohydrates to the SOM.

Melanin, another fungal cell wall component, is responsible for coloration in a variety of organisms, including fungi. In addition to coloration, melanin in fungal cell walls has been shown to protect fungal tissue from environmental stresses including UV damage, excess water, and toxic metals (Fernandez and Koide 2013; Gadd and de Rome 1988; Kogej, Gorbushina, and Gunde-Cimerman 2006; Singaravelan et al. 2008). This high molecular weight, hydrophobic, irregular biopolymer differs in structure from species to species (Nosanchuk, Stark, and Casadevall 2015). The biosynthetic pathway for melanin begins with indolic or phenolic precursors, leaving the final melanin product highly aromatic in structure (Butler and Day 1998). Fungi produce melanin through two major pathways, DHN and l-DOPA, which are named for key intermediates 1,8-dihydroxynaphthalene and L-3,4-dihydroxyphenylalanine, respectively (Eisenman and

Casadevall 2011). Melanin is thought to form regular layers within the cell wall that intertwine with other structural molecules for added strength (Casadevall et al. 2012; Eisenman et al. 2005; Zhong et al. 2008). Although melanin cannot be exactly characterized due to its structural complexity and species to species variation, melanin's presence is typically confirmed by characteristic electron paramagnetic resonance (EPR) behavior produced from the presence of unpaired electrons in the melanin structure (Enochs, Nilges, and Swartz 1993; Wang, Aisen, and Casadevall 1995).

Melanin has long been thought to be an important factor in fungal degradation. As described above, early studies have found higher melanin content to correlate to degradation resistance (Hurst and Wagner 1969; Linhares and Martin 1978; Malik and Haider 1982). More recently, it was shown that ectomycorrhizal fungal tissue degradation in forest soils was slowed by increasing melanin concentrations in the degrading fungal tissue (Fernandez and Koide 2014; Ryan 2019; Ryan et al. 2020). Clemmensen et al. (2015) also found that fungi with greater melanin concentrations correlated with greater SOM accumulation in forest soils.

Although the cell wall is generally considered to be resistant to fungal degradation, portions of the plasma membrane, including membrane sterols, can also be found preserved in sediment, indicating a potential long-term preservation of sterols in the environment (Nishimura and Koyama 1977). Ergosterol (ergosta-5,7,22-trien-3β-ol) is a sterol specific to fungal tissue that is found in all species in the same form (Bergmann and Klacsmann 1948; Nylund and Wallander 1992). Thus, the chemical structure of ergosterol is well characterized (Figure 1.5). This sterol is a small molecule with multiple ring structures which could make it resistant to degradation in natural soils. Additionally,

ergosterol forms a significant amount of living fungal biomass, ranging from 2.6 to 42 µg/mg dry mass (Pasanen et al. 1999).

1.3 Chemical analysis of OM

Chemical characterization of SOM with respect to fungal tissue poses an analytical challenge for many reasons, among them sample heterogeneity (Kögel-Knabner 2000; Simpson and Simpson 2012). One method that has been applied in a variety of studies is infrared spectroscopy, which can characterize the types of covalent bonds present in given sample based on the characteristic absorbance wavelength of these bonds. This technique has been applied to fractionated soil samples (Celi, Schnitzer, and Nègre 1997; Kang and Xing 2005) and degraded biological tissue (Joffre et al. 1992; Schreiner, Blair, and Levinson, William Egerton-Warburton 2014) to describe sample bulk characteristics. Nuclear magnetic resonance spectroscopy (NMR) allows investigation of the chemical bonds associated with NMR active atoms such as carbon-13 and nitrogen-15 and is commonly combined with IR techniques (Celi et al. 1997; Kang and Xing 2005). NMR techniques are especially popular in stable isotope studies where NMR can probe for differences in the environment of the labelled atom (Spence et al. 2011; Webster, Chudek, and Hopkins 1997).

In contrast to spectroscopy, which can give only non-quantitative information about the bulk characteristics of SOM, pyrolytic techniques combined with gas chromatography/mass spectrometry (GCMS) allows characterization and quantification of individual compounds within the bulk sample (Shadkami and Helleur 2010). Analytical pyrolysis GCMS is a volatilization technique used in coordination with GCMS

that causes thermal cleavage to volatilize analytes directly prior to the inlet of the GC. This technique allows analysis of large, bulky samples that are either too bulky to vaporize and send through a GC column or are not readily soluble in common GC solvents. Through excess thermal energy, analytical pyrolysis causes radical cleavage and rearrangement, with specific reactions dependent largely upon exact temperature (Sobeih, Baron, and Gonzalez-Rodriguez 2008). Kallenbach et al. (2016) used this technique to compare SOM created by different microbial sources and that of native soils. Microbially derived SOM exhibited a similar mixture of complex organic molecules as that of native field soils (Kallenbach, Frey, and Grandy 2016).

A related technique, thermochemolysis-GCMS, uses a basic alkylating reagent to further assist bond cleavage and allow analysis of highly polar functional groups in a standard, non-polar GC column. This technique is also referred to in the literature as chemopyrolysis and thermally assisted hydrolysis and methylation (THM) (Challinor 2001; Steinberg, Nemr, and Rudin 2008). Compared to analytical pyrolysis, thermochemolysis uses lower flash heating temperatures (300-600°C in thermochemolysis versus 400-700°C in pyrolysis) (Shadkami and Helleur 2010). These lower temperatures prevent cracking, or C-C bond breakage, that is common in pyrolysis. By methylating at nucleophilic sites, thermochemolysis prior to GC separation allows analysis of highly polar groups such as carboxylic acids and sugar molecules (Challinor 2001; Fabbri and Helleur 1999).

Thermochemolysis is accomplished with a suite of different alkylating reagents, though tetramethylammonium hydroxide (TMAH) is the most common, representing approximately 90% of the literature (Shadkami and Helleur 2010). Some other alkylating

agents include tetraethyl- and tetrabutyl-ammonium hydroxide that can be used to distinguish between added and preexisting methyl groups on the original polymer (Shadkami and Helleur 2010). Tetraethylammonium acetate (TEAAc) has been used alongside TMAH to distinguish between free and bound fatty acids in humic matter, as TEAAc will only alkylate free fatty acids whereas TMAH will alkylate free fatty acids and will also hydrolyze the ester bonds of bound fatty acids due to its stronger alkaline properties (Guignard, Lemée, and Amblès 2005). TMAH is preferred in analytical studies due to its strongly basic characteristic (pK_b 4.2), which minimizes substrate preferences, and its smaller molecular size which eliminates most steric effects which could be detrimental to its performance in the matrix (Lehtonen, Peuravuori, and Pihlaja 2003).

Previous studies have been successful in characterizing biological tissue and SOM using thermochemolysis or pyrolysis GCMS (Carr et al. 2013; Kallenbach et al. 2016; Ryan et al. 2020). Schwarzinger (2005) used thermochemolysis GCMS to identify characteristic peaks for different fungal groups and assign identifications based upon these chromatograms. Additionally, the toxin α-amanitin was also identified in the fungal thermochemolysis GCMS studies through similarity to an α-amanitin standard (Schwarzinger 2005). Sporopollenin in archived fungal spore samples has also been identified through thermochemolysis GCMS (Watson et al. 2007). One highly cited use for thermochemolysis GCMS with TMAH is the analysis of lignins in biological samples and SOM (Challinor 1995; Hatcher et al. 1995) Studies of SOM components have proven successful in a variety of different laboratories (Calderón, McCarty, and Reeves 2006; Kallenbach et al. 2016; Ryan et al. 2020; Xiong et al. 2019). Plant exudates under different warming conditions were successfully characterized through soil sample

thermochemolysis GCMS (Xiong et al. 2019). Recently, py-GCMS has been used to study the chemistry of soil microbial tissue (Kallenbach et al. 2016) and thermochemolysis GCMS has been used to study the chemistry of fungal tissue (Ryan 2019; Ryan et al. 2020). Ectomycorrhizal fungal necromass degradation was examined for chemical composition changes across a 90 day degradation chronosequence in forest soils (Ryan 2019; Ryan et al. 2020). Other organic matter degradation has also been examined using py-GCMS such as composting manure (Calderón et al. 2006).

Some of the biomolecule classes of interest to study have also been addressed in previous works. Fabbri and Helleur have published thermochemolysis behavior of simple and polymeric carbohydrates (1999). Thermochemolysis GCMS has also been used to positively identify both individual amino acids (Gallois, Templier, and Derenne 2007) and proteinaceous material from extracted soils (Zhang et al. 2001). Lipids have been studied successfully with this technique (Dworzanski et al. 1991; Xu, Basile, and Voorhees 2000), and by subjecting entire bacterial samples to this method, species identity could be determined through lipid thermochemolytic products (Xu et al. 2000).

1.4 Modeling of degradation data

Treating both specific biomolecules and bulk makeup of fungal tissue in parallel, one can characterize degradation behavior of fungal tissue. Classically, first order kinetics have been used to fit natural OM degradation beginning with Berner (1964) and Olson (1963). This agrees with the idea that degradation is accomplished by enzymatic action, which is typically modeled in a first order or pseudo-first order manner (Cornish-Bowden 1999). The first iteration of this model, termed the single-G model (Berner 1964;

Olson 1963), assumed that the organic carbon was depleted by one major first order reaction pathway such as the OM oxidation presented below (Rxn 1).

$CH_2O + O_2 \rightarrow CO_2 + H_2O$ (Rxn 1)

This reaction (Rxn 1) describes respiration using CH_2O as the empirical formula for OM. According to this reaction scheme, the mass of organic carbon, or CH_2O, will be depleted as O_2 is consumed. Two issues with using reaction 1 to model natural SOM degradation are (1) OM is composed of many different compounds and (2) different compounds degrade with different kinetic rates (Westrich and Berner 1984).

Subsequent revisions of this model, termed the "multi-G model," allow the amount of total organic carbon to be depleted by multiple major pathways hypothesized to depend on the differing chemical structure of the OM present (Westrich and Berner 1984). These multi-G models also typically include an unreactive pool of carbon, G_{nr}, with an unchanging total mass for the length of the experiment. Multi-G degradation typically takes the form of Equation 1 below assuming two reactive carbon fractions G_1 and G_2.

$$\frac{-dG}{dt} = k_1 G_1 + k_2 G_2 + G_{nr} \quad \text{(Eq 1)}$$

In Equation 1, the rate of change in the size of the total carbon pool (dG/dt) is related to the sum of the changing carbon sub pools (G_1 and G_2) whose rate of degradation is determined by kinetic rate constant for each pool (k_1 and k_2), and the non-reactive pool (G_{nr}) does not degrade. This equation is typically written with a higher k_1 value compared to k_2, indicating G_1 will degrade faster than G_2. Equation 1 can then be integrated over time to yield the following expression (Eq 2):

$$G_t = G_{1,0} e^{-k_1 t} + G_{2,0} e^{-k_2 t} + G_{nr} \quad \text{(Eq 2)}$$

In Equation 2, $G_{1,0}$ and $G_{2,0}$ refer to the original concentration of each fraction of OM at time zero, and G_t refers to the total organic carbon pool at time t. The derivation of this model assumes that the OM utilized in degradation must fall into groups categorized by the rate constants of their oxidation. It also assumes that degradation of OM only depends on the concentration of available OM. Although this model relies heavily on empirical fitting, with the existence of 5 fit parameters in Equation 2, a theoretical derivation of this model was proposed by Boudreau based on surface area available for microbial enzymatic attack (1992). Single and multi-G degradation has been shown to fit degradation data well from many different environments and of many different types, and has thus continued to make appearances in the literature (*e.g.* Bryant et al. 1998; Ryan et al. 2020; Harmon et al. 2009; Bontti et al. 2009).

1.5 Organization of this document

In this thesis, I detail the chemical characteristics of saprotrophic fungal degradation. Chapter 2 is written in a style for future publication and Chapter 3 contains an appendix of supporting data taken during method development as well as detailed laboratory protocols for my data collection and analysis methods. The nature of this organization requires repetition in introductory literature analysis and procedural details in Chapters 2 and 3. For Chapter 2, I derive degradation constants for comparison to literature values and also show the dynamic chemical changes that occur along a degradation chronosequence. The methods developed for this study are intended to form foundational SOPs for the laboratory group to be used in future studies and the

results presented in this paper will contribute to grow the body of knowledge regarding fungal saprotroph degradation as a wildly underrepresented group of inputs to the soils.

CHAPTER TWO

2.1 Introduction

Worldwide, the top meter of terrestrial soil contains approximately 1500 Pg of carbon, twice that which exists as carbon dioxide in the atmosphere (Bernhardt and Schlesinger 2013). Through fixation, degradation, and respiration, soil organic matter (SOM) is linked to carbon dioxide and methane in the atmosphere, both of which are a major factor in anthropogenic global warming (IPCC 2013). Multiple mathematical models have aimed at describing soil processes and interaction with climate (Manzoni and Porporato 2009) though commonly used models have poor descriptive capability when extrapolated over time and space (Todd-Brown et al. 2013). Soil carbon cycling is a difficult problem to address mathematically due to the large number of interacting processes such as oxygen infiltration, carbon dioxide effusion, root respiration, microbial turnover, and water transport through structurally heterogeneous soils, for which the rate of each process relies on others in addition to external factors such as soil temperature and precipitation events (Blagodatsky and Smith 2012). Furthermore, complete chemical characterization of SOM is difficult the large macromolecular structures of OM that are asymmetric and irregular (Hedges et al. 2000). Because the source and chemistry of SOM has yet to be fully understood, the fate of this carbon pool is also uncertain in a changing climate. As such, it is important to characterize and understand the chemical reactions that control fluxes of the SOM pool to make future climate predictions (Simpson and Simpson 2012).

Historically, long-lived SOM was thought to be a heteropolymer that could be isolated from the soils. Both stable SOM substances and lignin, a well-known plant

heteropolymer, were operationally defined by harsh extraction techniques (Burges et al. 1964; Piccolo et al. 2002). These extraction and isolation methods identify substances of similar molecular weight and aromaticity for SOM and lignin(Burges et al. 1964; Piccolo et al. 2002). The majority of OM degradation literature has thus been focused on the lifetimes and chemical makeup of degrading plant tissues. However, this paradigm is beginning to shift with the discarding of old SOM isolation protocols and the adoption of whole soil bulk chemical analysis methods. For example, whole soil NMR, FTIR, and pyrolysis GCMS analysis have found remarkable overlap with microbial OM (Kallenbach et al. 2016; Ryan et al. 2020; Simpson et al. 2007) suggesting 50% of SOM could be microbially derived (Simpson et al. 2007).

Increasingly, microbes are thought to play an important role in SOM turnover and formation (Miltner et al. 2011; Simpson et al. 2007). Fungi specifically are known to decompose all common biopolymers, making them important processors of current and future SOM (Baldrian et al. 2010). Indeed, it has been shown that carbon added to the SOM pool is primarily processed by fungi first (Godbold et al. 2006). Fungal hyphae are also known to form soil aggregates, contributing to SOM stabilization (Six et al. 2006). Microbial tissue itself is increasingly thought to be a significant source for long-lived SOM (Liang et al. 2010). Other studies have examined the chemistry of SOM and have determined that much of the chemistry of SOM resembles fresh microbial tissue (Kallenbach et al. 2016; Spence et al. 2011).

Degradation of fungal tissue has been found to be slower compared to bacterial biopolymer degradation (Guggenberger et al. 1999). Although fungal tissues are made up of a diverse mix of polymers and small molecules which are mixed in different ratios,

some specific degradation drivers have already been elucidated such as nitrogen content, OM complexes, and the presence of specific biopolymers (Adamczyk et al. 2019; Koide and Malcolm 2009; Ryan et al. 2020). Similar to plant litter, degradation rates of fungal tissue have been shown to depend on tissue nitrogen content (Koide and Malcolm 2009), in which tissue with higher relative amounts of nitrogen is degraded faster (Ryan et al. 2020). Fungal tissue degradation can be environmentally controlled as is seen when secreted plant tannins complex with fungal tissues to form OM resistant to degradation (Adamczyk et al. 2019). Fungal melanin molecules produced withing the fungal tissue itself can also chemically resist degradation (Butler and Day 1998; Linhares and Martin 1978) and fungal tissues containing melanin have shown to persist longer in the environment than tissues without melanin suggesting melanin itself protects the associated tissues (Fernandez et al. 2019; Ryan et al. 2020). Fungal degradation studies have largely focused on plant-associated fungal species (ECM) in forest (Fernandez and Koide 2012; Godbold et al. 2006; Ryan et al. 2020) or peatland soils (Fernandez et al. 2019). Since factors shown to control degradation are associated with the fungal chemical composition (such as nitrogen or melanin content) or the fungal environment (such as the availability of plant tannins), it is important to carefully consider different fungal families and ecosystems when reviewing SOM degradation.

Recently, thermochemolysis gas chromatography/mass spectrometry (GCMS) has been used to analyze various types of complicated organic matter for its specific chemical constituents, including whole soils (Schulten and Sorge 1995), extracted soil fluvic acids (Lehtonen et al. 2003), and fungal necromass (Ryan et al. 2020). This technique uses basic alkylation and increased temperatures to break apart large molecules prior to

introduction to the GCMS system (Shadkami and Helleur 2010). GCMS provides separation and detection capable of assigning individual compound identities while thermochemolysis prepares large and polar molecules for such an analysis. When compared to NMR or FTIR techniques which are also used to chemically characterize complex natural mixtures (Schreiner et al. 2014; Simpson et al. 2007), thermochemolysis is a more detailed technique and can reveal individual compounds (Kögel-Knabner 2000). Pyrolysis at higher temperatures and without additional chemical catalysis has also been used to study SOM and examine potential microbial sources (Kallenbach et al. 2016).

In this study, we examine the degradation of four saprotrophic fungal species for bulk and individual chemical behavior. The results from this study represent the first numerically modeled saprotrophic fungal tissue decay sequence and detailed chemical study of degrading saprotrophic fungal tissue in a grassland ecosystem. We describe the kinetic degradation of the total mass over a 28 day period using a single- and multi-G model (Berner 1964; Olson 1963; Westrich and Berner 1984). Detailed chemical analyses of the degrading tissue are completed using thermochemolysis gas chromatography/mass spectrometry (GCMS). This technique elucidates the dynamic chemical changes that occur during this degradation period and interrogate possible portions of the necromass that may contribute to long-lived SOM.

2.2 Methods

Fungal decay experiments

Fungal decay experiments were completed on the necromass of four saprotrophic, ascomycete fungal species: *Fusarium avenaceum, Hydnotrya, Xylaria* spp., and an unidentified, highly pigmented *Ascomycota* (Hemiascomycete). The unidentified *Ascomycota* was propagated from fungi growing on the surface of an *Artocarpus* (jackfruit) leaf growing in the Chicago Botanic Garden greenhouse, Glencoe, IL (42° 8' 28" N, 87° 47' 14" W). The *Xylaria* species was cultured from the persistent spores found on the surface of a *Melangoster* sp. fruiting body collected in the Yucatan peninsula. The *F. avenaceum* and *Hydnotrya* species were each cultured from Illinois soil samples collected from the first 10 cm of the prairies and oak-maple forests, respectively, on the grounds of the Chicago Botanic Garden.

Fungi were all serial cultured on Potato Dextrose Agar plates (PDA; 39 g/L) to obtain single-strain cultures. For soil-derived fungi, the soil samples were first diluted to a concentration of 10 g/L with sterile deionized water and filtered to remove large soil particles. The soil solutions were then directly applied to the PDA plates and all plates were incubated at room temperature (22°C). High density cultures were achieved using 30 replicate flasks of 200 mL of sterile, liquid Tryptic Soy broth inoculated with a 2 mm plug of fungal culture. After incubation produced enough tissue (14 days *F. avenaceum*, 21 days all other species), fungal tissue was harvested and washed with carbon-free water to remove culture media, freeze-dried, and weighed. Approximately 250-300 mg of fungal tissue was placed in 4 cm^2 stainless steel packets (pore size 100 µm, Vacco Industries). *Hydnotrya* cultures did not proliferate to the same extent as the other species producing fewer packets which were sampled less frequently.

Fungal tissue samples were buried in temperate prairie soil at the Chicago Botanic Garden in adjacent 10 cm x 10 cm plots. Each sample was buried 5-10 cm below the soil surface while disturbing the pants and soil as little as possible. *F. avenaceum* samples were buried in the summer of 2013 while *Hydnotrya, Xylaria* spp., and the *Ascomycota* species were buried in the summer of 2014 when precipitation and temperature from the Chicago Botanic Garden weather station showed similar conditions. The packets were left for the fungal tissue to degrade over a 28-day period and harvested in triplicate at days 1, 2, 4, 7, 14, and 28 (*Hydnotrya* sampled at 1, 2, 7, and 28; *F. avenaceum* was sampled an additional time at day 21). Control packets were also sampled on the same day after burial to represent the tissue at day 0 and account for any disturbances caused by the burial process. Packets chosen for harvest were determined using a random number generator. After harvest, packets were freeze dried, weighed, and tissue was scraped out and homogenized with mortar and pestle.

Analysis of fungal tissue

To determine the changing chemistry of fungal necromass during decay, elemental analysis-isotope ratio mass spectrometry (EA-IRMS) was carried out at Northwestern University Earth and Planetary Sciences Stable Isotope Facility. A Thermo Delta V isotope ratio mass spectrometer interfaced with a Costech EA 4010 by a Conflo IV interface was used to complete the elemental analysis. Standard deviation of internal lab standards was approximately 0.28% for %C and %N. Standard deviations between field replicates were also calculated and reported.

Thermochemolysis pyrolysis-GCMS (py-GCMS) analyses was also completed on fungal tissue. Tissue consisting of approximately 70 µg organic carbon was combined with 15 µL of 25% tetramethyl ammonium hydroxide (TMAH) in methanol (Sigma) in a quartz pyrolysis tube. The sample was then heated to 300°C at a rate of 720°C/min using a Gerstel Thermal Desorption Unit and pyrolyzer. Volatilized sample entered the silica GC column (Agilent Technologies, HP-5MS, 30 m by 0.250 mm) where GC oven (Agilent Technologies, 7890B) temperature was ramped from 50°C to 320°C over a period of 50 minutes with a 10-minute heated final hold. Compounds were ionized within the mass spectrometer (Agilent Technologies, 5977A) using a voltage of 70 eV.

Compounds within pyrograms were identified based on similarity to standards, published thermochemolytic data (Fabbri and Helleur 1999), and NIST identity. Standards used for analysis included mannan (isolated from *Saccharomyces cerevisiae* via alkaline extraction, Sigma), β-glucan (isolated from *Saccharomyces cerevisiae*, Sigma), and chitin (isolated from shrimp shells, Sigma). Peaks representing >1% relative abundance for each chromatogram were integrated via extracted ion chromatogram (EIC) at the m/z of interest by MassHunter software. A total of 148 compounds were identified among the data for all four species.

2.3 Results

The total dry mass, organic carbon, and nitrogen of the fungal tissue is shown to decay rapidly within the first week and then more gradually for the remaining time period (Figure 2.1). The bulk mass, organic carbon, and nitrogen values are all visualized as a ratio to the day 0 amounts (Figure 2.1). In some cases, the value of a degraded sample

was greater than that of the day 0 sample. This may occur due to mineral leaching into the packets or ingrowth into the mesh. Values for bulk mass, organic carbon, and nitrogen all represent averages of multiple field replicates. Where values represent the average of multiple field replicates, the standard error and number of samples analyzed (N) are reported. The average total mass falls to less than half across the 28-day period (*F. avenaceum*, 30.8%, error 4.96%, N=3; *Hydnotrya*, 48.3%, error 43.4%, N=4; *Xylaria*, 25.2%, error 19.5%, N=3; *Ascomycota*, 12.0%, error 4.89%, N=4). This behavior is overlaid with a single exponential function for the total mass loss (Figure 2.1a). The decrease in organic carbon and total nitrogen are also represented in Figure 2.1b and Figure 2.1c respectively. The average total carbon content falls across the experiment time period to a percentage of the original (*F. avenaceum*, 74.1%, error 4.40%, N=3; *Hydnotrya*, 44.0%, error 2.37%, N=4; *Xylaria*, 15.2% error 6.60%, N=3; *Ascomycota*, 6.3%, error 1.44%, N=3). The decrease in carbon is similar to the decrease in nitrogen content closely for all species (*F. avenaceum*, 65.8%, error 4.92%, N=3; *Hydnotrya*, 50.6%, error 3.23%, N=4; *Xylaria*, 14.6%, error 4.87%, N=3; *Ascomycota*, 6.0%, error 1.04%, N=3). At intermediate timepoints, the *Xylaria* species does show a mismatch in carbon and nitrogen degradation extent as shown by the intermediate increase of C/N ratio for the *Xylaria* species (Table 2.3). The *Hydnotrya* species has the largest C/N ratio at the beginning of the study and is the only species in which the C/N ratio decreases across the degradation period (Table 2.3). The decrease in carbon and nitrogen closely mirror the behavior of the total mass.

The chemical composition of the degrading tissue was examined by TMAH py-GCMS (Figure 2.2-2.5; Table 2.4). The changes in fungal tissue chemistry over the first

two-week period are dynamic. The lipid component changes within the first week from day 0 values (*F. avenaceum*, 18.03%, *Hydnotrya*, 31.07%, error 10.55%, N=3; *Xylaria*, 25.20%; *Ascomycota*, 63.50%, error 8.94%, N=3) and then lipid component values stabilize for the last two week of the study with ending mass percentages all approximately 20% (*F. avenaceum*, 23.57%; *Hydnotrya*, 20.42%, error 2%, N=3; *Xylaria*, 17.64%, error 1.68%, N=3; *Ascomycota*, 28.12%). For all species, the lipid component degrades to a greater extent than the rest of the components except for *F. avenaceum* which had marginal increase in average lipid relative composition at the end of the 28-day study. The sterol component of the total fungal tissue increases with time for every species from day 0 (*F. avenaceum*, 0.79%; *Hydnotrya*, 0.63%, error 0.27%, N=3; *Xylaria*, 0.67%; *Ascomycota*, 1.86%, error 1.10%, N=3) to day 28 (*F. avenaceum*, 11.50%; *Hydnotrya*, 11.96%, error 3.54%, N=3; *Xylaria*, 1.84%, error 0.95%, N=3; *Ascomycota*, 4.84%). The aromatic fraction of the total fungal tissue changes differently across species from day 0 (*F. avenaceum*, 4.20%; *Hydnotrya*, 31.26%, error 46.32%, N=3; *Xylaria*, 9.56%; *Ascomycota*, 3.24%, error 0.61%, N=3) to day 28 (*F. avenaceum*, 5.90%; *Hydnotrya*, 3.22%, error 0.67%, N=3; *Xylaria*, 8.36%, error 1.28%, N=3; *Ascomycota*, 9.82%). Nitrogen-containing fractions of the total tissue also change in differently across species from day 0 (*F. avenaceum*, 35.77%; *Hydnotrya*, 6.81%, error 5.08%, N=3; *Xylaria*, 9.61%; *Ascomycota*, 4.78%, error 1.61%, N=3) to day 28 (*F. avenaceum*. 9.01%; *Hydnotrya*, 35.9%, error 6.13%, N=3; *Xylaria*, 3.70%, error 0.66%, N=3; *Ascomycota*, 8.15%). However, both aromatic and N-containing moieties end the study making up less than 10% of the detected fungal compounds by peak area, with the exception of *Hydnotrya* which ends the study with a large portion of nitrogen

compounds. The portion of unspecified compounds at the end of the study (*F. avenaceum*, 14.62%; *Hydnotrya*, 8.06%, error 0.98%, N=3; *Xylaria*, 12.65%, error 2.54%, N=3; *Ascomycota*, 11.94%) is more than at day 0 (*F. avenaceum*, 7.55%; *Hydnotrya*, 2.14%, error 0.87%, N=3; *Xylaria*, 6.13%; *Ascomycota*, 0.55%, error 0.39%, N=3). Over the course of the degradation chronosequence, the carbohydrate or sugar component increases in concentration for the biomass for *F. avenaceum* and *Xylaria* (day 0: 33.64% and 48.84%; day 28: 35.41% and 55.81%, error 5.53%, N=3). *Hydnotrya* tissue experiences a slight decrease in sugar composition from day 0 (28.10%, error 15.24%, N=3) to day 28 (20.44%, error 4.48%, N=3), whereas the *Ascomycota* tissue experiences a slight concentration of sugar component from day 0 (26.08%, error 4.31, N=3) to day 28 (37.13%).

2.4 Discussion

Bulk kinetic analysis

The single G model is based on simple first order kinetic consumption of organic carbon [G]. This model is arguably the simplest way to model degradation behavior and has been in use since its conception (Berner 1964; Olson 1963). This model states that the rate of consumption of G is directly proportional to the rate constant k and the concentration of G while the consumption of G follows first order kinetics (Equation 3).

$$\frac{G_t}{G_0} = e^{-kt} \qquad \text{(Eq 3)}$$

In Equation 3, carbon mass at time t (G_t) is normalized to the initial mass (G_0). This ratio displays an exponential dependence on the time variable that is scaled by the kinetic rate constant k. Equation 3 is fit to the experimental data directly (Figure 2.1).

An extension of the single G model is the double G model which uses the same simple understanding of first order kinetics and expands upon it to describe more than one pool of degrading carbon (Westrich and Berner 1984). This model allows for better empirical fit of the natural carbon pool as SOM is not composed of a singular carbon source or chemical makeup. A double G model is employed to model the data in this study as described in Equation 4 below.

$$G_t = G_{1,0} e^{-k_1 t} + G_{2,0}\, e^{-k_2 t} \quad \text{(Eq 4)}$$

In equation 4, carbon pool 1, or G_1, is controlled by kinetic constant k_1 and is a fast degrading pool. Once carbon pool 1 is mostly or completely degraded away, the rate of the total carbon degradation slows corresponding to a slower rate constant assigned to the remaining carbon that forms carbon pool 2, G_2. These two pools represent the heterogeneity of natural OM and are used to help approximate degradation rates (Westrich and Berner 1984). The degradation of pool 1 and pool 2 happen in parallel and both contribute to the rate of the overall carbon loss as described in Equation 4 (Table 2.1).

As is shown in Figure 2.1, a single exponential model fits the data best for the first two weeks of decay with decreasing ability to predict the later time points. A double G model was also fit to this data and both model fits are summarized in Table 2.1 (except for the *Hydnotrya* species which was unable to fit due to the decreased sample density). All fungal species have degradation kinetic coefficients, k, similar in magnitude for

each the single G model (k range from 0.0503-0.167 day^{-1}) and double G (k_1 range from 0.171 to 0.297 day^{-1}; k_2 range from 0.00899 to 0.0303 day^{-1}). The turnover time is reported as the inverse of k for another representation of the data (Table 1). Although the data is well fit by these G models, it is important to consider that the rate constants presented in this study are based on the assumption of one or two finite pools of organic matter and are biased by the time scale of the experiment. As litter inputs are heterogeneous in chemical nature, and uncontrolled environmental processes affect and control the rate and extent of degradation, the use of mathematical models will not capture the full complexity of the system. Furthermore, the time scale or data density from this experiment may also affect the data when approximating the inflection point in a double G model or assuming that the material continues to degrade according to the same kinetic constants beyond the 28 day chronosequence that was sampled. The single and double G values are merely an attempt to characterize the rate of degradation in a common form that will be easily comparable to other literature values.

With soils containing such a significant portion of carbon in the global system, it is important to fully understand the degradation resistance and lifetime of SOM. Soil carbon models are frequently used to model reactions or fluxes of carbon within different pools in soils (Parton et al. 1998; Skjemstad et al. 2004; Zimmermann et al. 2007). These models can then predict with varying accuracy how soil carbon fluxes and storage will be altered with changing climate variables. However, the accuracy of these models is dependent on the underlying assumptions and the data used to calibrate these models.

Two of the most well-cited models are the RothC (Coleman and Jenkinson 1996) and CENTURY (Campbell and Paustian 2015; Parton et al. 1993). These models are both

multi-pool representations of carbon soil cycling. CENTURY and RothC both focus on the incoming plant residues as sources of the passive or resistant SOM with microbial pools as intermediary (Campbell and Paustian 2015; Coleman and Jenkinson 1996; Parton et al. 1993). The microbial biomass degradation constant calculated from the RothC and CENTURY models are between 0.00182 day^{-1} to 0.00198 day^{-1} (Cong et al. 2014; Jenkinson et al. 1990; Morais, Teixeira, and Domingos 2019; Parton et al. 1993). The degradation in these models are one to two orders of magnitude lower than all the measured fungal constants reported for saprotrophic decay in this study (Table 2.1).

The bulk saprotrophic fungal mass in this study quickly degrades within the first week before the degradation rate slows significantly, approaching zero at the end of the study. Initial fast cycling kinetics are seen for other fungal tissue (Ryan et al. 2020) as well as plant tissues (Webster and Benfield 1986). Recently, a laboratory study has shown that microbial mass can be quickly lost (25-50% in one day) to abiotic leaching (Maillard et al. 2020) which could contribute to fast initial necromass degradation in soil experiments to an unknown degree. The slow cycling kinetic rate may also be biased fast by the short timeframe of the study as it has been shown that little fungal degradation occurs after a 1-mong time window (Fernandez et al. 2019; Ryan et al. 2020). A longer time study may therefore deemphasize the early, fast-cycling kinetics and may achieve a more accurate estimation of the slow-cycling kinetic. In this way, the time length of the study must be considered when comparing to the literature.

While much faster than allowed for in SOM models, the bulk fungal tissue degradation rates reported in this study are also faster than what is shown in degradation studies of other types of tissue. Bulk degradation of plant tissues has been found to be

significantly slower by Melillo et al. (1982) with kinetic rate constants 1-2 orders of magnitude smaller (k values of roughly 0.0013 to 0.00022 day^{-1}). Microbial tissue from similar degradation studies have shown greater overall persistence than the fungal tissue degradation reported in this study (Follett, Paul, and Pruessner 2007; Paul et al. 2011). Studies of fungal tissue show fungal matter persists within the natural environment for 28 days and longer (Certano et al. 2018; Ryan et al. 2020). The discrepancies between these bulk microbial tissue studies and the data presented here may be due to the use of carbon isotope labelled biomass, rather than the litter bag model employed in this study. Litter bag studies, including the data presented here, are performed in a manner where the degrading tissues are unable to interact with the soil matrix and form physical associations that may protect the tissue from degradation in a manner that offers physical protections from degradation (Six et al. 2006). Ryan et al. (2020) studied ectomycorrhizal fungal tissue over a 90-day period and reported kinetic rate constants for the single G model between 0.0146-0.0436 day^{-1}. Despite differences when compared to literature isotope studies, litter bag technique was chosen for this study to enable the recovery of saprotrophic necromass for chemical analysis. However, Voroney and Paul (1984) used an isotope label to determine microbial turnover times to be approximately 7.7 days which is directly comparable to the fungal turnover times presented here. This suggests that other complicating factors exist in direct study comparisons which may include soil clay content, precipitation, or temperature during study period.

Nitrogen loss within fungal tissue

Fungal tissue nitrogen degradation proceeds in the same exponential loss pattern as the total mass loss across the degradation chronosequence (Figure 2.1). Single G modeling was carried out for the nitrogen and carbon degradation (Table 2.2). In all species, the nitrogen degradation kinetics are faster than the carbon kinetics, but not necessarily faster than the bulk degradation kinetics. Microbial tissue has other elements incorporated such as hydrogen, oxygen, sulfur, phosphorus which contribute roughly half of the total mass so these other elements could also affect differences in the bulk tissue mass kinetics (Duboc et al. 1995). Thermochemolysis py-GCMS also shows a slight increase in relative concentration of nitrogen containing compounds within the fungal tissue for all species by day 28 (Figures 2.2-2.5).

A similar extent of nitrogen loss has been reported in the literature. C-14 labelled free amino acids and purified peptides applied to soils and left to degrade in the environment lost 71-90% of the carbon label over a 4-week period (Verma, Martin, and Haider 1975). Other studies on whole soils found long-term stability of amide nitrogen suggesting proteins do not completely degrade, though they might be incorporated into other biomass (Miltner et al. 2009; Spence et al. 2011). Fungal tissue specifically has shown nitrogen compounds remain and are enriched after a degradation chronosequence (Ryan et al. 2020). The fungal degradation data presented here also shows nitrogen compounds persist within the degraded day 28 necromass for all species. This is also shown in the C:N ratio during the degradation sequence for these species, with stable C:N ratio (Table 2.3) with the exception of the nitrogen in *Hydnotrya* (day 0 C:N ratio, 8.729; day 28 C:N ratio, 7.472). Finally, this is also represented in the relative enrichment in pyrolytic nitrogen containing compounds for *Hydnotrya* and *Ascomycota*.

Overall changes to the C:N bulk elemental ratios can be viewed in the context of nitrogen depletion where the C:N value increase corresponds to a nitrogen depletion (Table 2.3). The C:N bulk depletion occurs in all species except for *Hydnotrya* where nitrogen is instead enriched at the end of the 28-day period. This enrichment trend is also seen in the pyrolytic data for the *Hydnotrya*. *Hydnotrya* has a high initial carbon content (Day 0 C:N ratio: 8.729) and a high initial aromatic content (Day 0 aromatic 31.26%, error 46.32%, N=3) which could act to protect the nitrogen based on the structural location of nitrogen-bearing chemical constituents.

For day 0 and day 28, overall changes in the bulk nitrogen data (C:N ratios, Table 2.3) and trends in the pyrolytic data (N-containing compound peak ratios, Table 2.4) are seen to correlate for all species except for *Ascomycota* (increasing C:N ratio: 6.137 to 6.406; increasing N-containing peak ratio: 4.78%, error 1.61%, N=3 to 8.15%). This discrepancy in the *Ascomycota* could be an artifact of nitrogen compounds depositing into the litter bag. Soil leaching and deposition is known to affect litterbag studies (Maillard et al. 2020; Tietema and Wessel 1994) and some compounds of both inorganic and organic nitrogen would be small enough to pass through the mesh pores of the litter bags in this study.

Studies have previously shown that nitrogen containing organic compounds degrade within the soils (Verma et al. 1975) which would agree with this study's observed total nitrogen loss from bulk tissue in all species. Further, all species show preferential degradation of nitrogen through faster nitrogen degradation kinetics as compared to carbon degradation kinetics (Table 2.2). By the end of the study *F. avenaceum*, *Xylaria*, and *Ascomycota* (all species except for *Hydnotrya*) show

preferential degradation of the nitrogen component of the tissue through increasing C:N ratios.

It is also thought that high initial nitrogen composition correlates to more complete degradation (Koide and Malcolm, 2009). As shown in Figure 2.6,, the *Ascomycota* with the lowest C:N ratio (or highest relative nitrogen concentration) shows the smallest fraction of total mass remaining, but it has the slowest initial bulk degradation k_1 value recorded in this study (k_1=0.171). Interestingly, the fastest initial bulk degradation is seen for the *Xylaria* tissue (k_1=0.299 day^{-1}) which has a high initial C:N ratio (8.198). Potentially, this slow degradation in high nitrogen content *Ascomycota* tissue and fast degradation in high carbon content *Xylaria* tissue could be phenomena that our study uniquely characterizes due to the early sampling density. By the end of the degradation period, the data does show that high nitrogen content *Ascomycota* has the least remaining total tissue (Day 28, 0.121 ratio mass remaining). The *Ascomycota* has a high initial lipid component (Day 0 lipid, 63.50%, error 8.94%, N=3) which could indicate a waxy or hydrophobic layer acting to protect the tissue from degradation. This lipid component continues to form a majority of the pyrolytic compounds until the very end of the study (Day 28 lipid, 28.12%). This interesting dynamic where the extent of the degradation relates to the C:N ratios of the initial tissues but the rate of the degradation could be a deviation from other observations in the literature due to the previous studies not capturing the early degradation in their sampling schemes. Litter inputs are one of the main sources of nutrients and chemicals available for uptake in the soils and so understanding their fast cycling components can lead to better understanding of available nutrient for future growth of biomass.

Chemical changes in degrading fungal tissue during degradation

Themochemolysis py-GCMS of fungal tissue shows significant similarities between degraded necromass and bulk SOM. Pyrograms of SOM composition in arid and semi-arid shrub-lands as completed by Carr et al. (2013) show aliphatic percentage compositions between 20-35%; however, Kallenbach et al. (2016) found much lower aliphatic content in natural Montmorillonite soil with less than 10% total organic matter composition (Figure 2.7). The tissue in this study at Day 28 more closely represent the aliphatic content of shrub-lands than the temperate Montmorillonite sampled by Kallenbach et al. (2016). The polysaccharide composition measured in shrub-land soils (5-20%, Carr et al., 2013) is much smaller than measured at the end of the 28 day degradation period reported here for all species (20-55%) and that was found by Kallenbach et al. (~25%, 2016) which may reflect a preference for polysaccharides preservation in wet, temperate soils. Differences reported here may also reflect the differences in analytical technique as thermochemolysis py-GCMS has been shown to produce aromatic residues derived from polysaccharides (Fabbri and Helleur 1999), which may in turn increase aromatic detection while decreasing polysaccharide detection through differential peak assignment. Technique differences may make the data appear artificially dissimilar from literature values. Recently, Ryan et al (2020), used thermochemolysis py-GCMS data from degraded fungal tissues and native forest soils to show that the thermochemolytic composition of 90-day old fungal tissue approached the composition of SOM and estimated an period of 3 months to 7 years would be needed for fungal tissue to resemble SOM signatures. Although the exact thermochemolytic py-

GCMS of the native grassland soils was not measured in this study, the saprotrophic fungal tissue components are shown to increase in similarity to other native soil signatures in Figure 2.7.

Fungal sugar-derived compounds are shown to change dynamically across the degradation chronosequence and still make up a relatively large percent of the total fungal tissue at the end of the 28-day period. In previous studies, fungal sugars, including chitin and glucose derivatives, have been found to degrade rapidly compared to the rest of the fungal tissue with the fastest degradation occurring within the first week (Drigo et al. 2012; Fernandez and Koide 2012). Ryan et al. (2020) found a majority of fungal species experienced a rapid 50% carbohydrate loss with a portion of the necromass carbohydrates remaining after 90 days. Our saprotrophic fungal data shows a similar species-specific sugar degradation pattern where *Xylaria* and the *Ascomycota* tissue has stable sugar composition within the first week. *Hydnotrya* tissues sees a concentration of the sugar component and *F. avenaceum* tissue sees a degradation of the sugar component. This may suggest that saprotrophic fungal tissue from *F. avenaceum, Xylaria,* and *Ascomycota* behave similarly to microbial sugars, which are believed to constitute a stable portion of SOC (Glaser et al. 2004; Roberts and Jones 2012; Tsai et al. 1997). Furthermore, amino sugars (such as fungal chitin) are thought to be stabilized within soils (Glaser et al. 2004). Our data supports this in that the sugar composition makes up a significant portion of the biomass at the end of the study, and that the nitrogen containing compounds are stable over the last two weeks of the experiment, suggesting a steady state has been reached within the soil environment.

Overall, the persistence of the fungal tissue until the end of the 28-day period as well as the modelled persistent carbon pool of the double-G model suggests that some fungal tissue might be chemically stable within the soils for relatively long periods of time. The chemical constituents of the fungal tissue as measured by pyrolysis are also similar to bulk SOM, indicating they could contribute a significant amount of OM to long-lived SOM pools (Carr et al. 2013; Kallenbach et al. 2016).

Environmental Changes

Environmental changes are occurring within the Anthropocene that continue to alter and affect global nutrient cycling and overall SOM storage and dynamics. Up to 35% of the terrestrial biome may already be devoted to agriculture (Betts et al. 2007). As the global human population continues to grow, so does the demand for cultivated food. Classic styles of cultivation include tillage processes which are known to release carbon and nutrients from the soil and decrease overall SOM storage (Mann 1986; Darmody and Peck 1997). Under tillage cultivation practices, temperate grassland total microbial biomass is shown to decrease (Cotton and Acosta-Martínez 2018). Furthermore, fungal structures are disrupted and the fungal-to-bacterial ratio is shown to decrease (Frey, Elliott, and Paustian 1999; Strickland and Rousk 2010). The mechanical breakdown of fungal structures could also contribute to increase rate of fungal necromass degradation through damaging the tissues (Helgason, Walley, and Germida 2009). With land use changes causing soil disruptions that break down the tissues of fungi and any protective soil structures, it is likely that saprotrophic fungal-derived SOM would be susceptible to further degradation as many of the chemical structures left behind belong to the

polysaccharide, N-containing, and even certain lipid groups, such as fatty acids, have been posited to be easy energy sources for other soil microbes (Calderón et al. 2006; Drigo et al. 2012; Fernandez and Koide 2012; Koide and Malcolm 2009).

Global climate change continues to cause warming temperatures worldwide but the effect of climate change on fungal abundance and soil microbial ecosystems is inconclusive. Under artificially increased soil temperature conditions, total soil microbial biomass has been shown to decrease and the soil fungal markers or fungal relative abundance are also shown to decrease (Frey et al. 2008; Waldrop and Firestone 2004). Another changing environmental variable is the increasing atmospheric CO_2 levels (IPCC. 2013). Under atmospheric carbon chamber and Free-Air CO_2 Enrichment (FACE) studies, fungal abundance in forest and grassland ecosystems has been shown to increase under conditions of increased CO2 in the air above the sampled soils (Klamer et al. 2002; Phillips et al. 2002; Rillig, Christopher, and Allen 1999). Potentially this has to do with other environmental variables such as soil moisture or pH.

Another factor affecting fungi prevalence would be the expected shift from C3 to C4 communities under climate change scenarios (Taub 2010). As ecosystems shift away from C3, or woody, plants, the unique niche of the saprotrophic fungi in lignin degradation and its importance would be diminished with decreasing lignin in the litter of C4 plants (Dornbush et al. 2008). Forest soil microbial communities have shown an average increased fungal dominance on the whole when compared with grassland soil microbial communities but the native data have been shown to overlap (Joergensen and Wichern 2008). Decreasing fungal concentrations with changing primary producer ecosystems has been widely hypothesized but short term studies have failed to see these

effects under forced ecosystem succession from C3 to C4 (Marshall, McLaren, and Turkington 2011) as the soil microbial community is well buffered from aboveground inputs via already available soil nutrients (Moore et al. 2004). In this way, the fungal communities may be resistant to changes and the findings of this study would continue to be relevant despite expected changes to ecosystem litter inputs.

2.5 Conclusions

Saprotrophic fungal necromass is largely overlooked in the degradation literature. However, it exhibits short-term, fast cycling dynamics followed by long-term, tissue persistence that should be better incorporated into current soil carbon modelling. This complexity is currently not reflected in the soil carbon models and needs to be addressed. A significant portion of fungal tissue also persists in the environment after a 28-day degradation period, suggesting this tissue may join the long-lived SOM pool. Based on the data summarized here, this stable portion is likely polysaccharide and sterol rich and is chemically similar to bulk SOM.

CHAPTER 3

3.1 Fungal melanin extraction

Reference: Prados-Rosales et al, 2015

Chemicals List

PBS, Buffer A: 1M sorbitol/0.1M sodium citrate/pH 5.5, Buffer B: 10mM TrisHCl (pH 8.0)/5mM $CaCl_2$/5% SDS, Cell wall lysing enzyme from *Trichoderma harzianum* (*Sigma L1412*), 4M guanidine thiocyanate, Proteinase K (*Biological source unspecified*), Chloroform:methanol, 2:1

Method

1. Obtain and weigh freeze-dried fungal powder.
2. Dissolve in PBS.
3. Add Buffer A and lysing enzyme (10 mg/mL) and incubate at 30˚C for 24 hours.
4. Centrifuge at 3000 rpm for 10 min to collect cells and wash with PBS until supernatant is clear.
5. Add 1 mL of 4M guanidine thiocyanate and rock at room temperature for 12 hours.
6. Centrifuge to collect pellet and wash 2-3 times with PBS.
7. Add 1 mL Buffer B with proteinase K (final concentration of 1mg/mL) and incubate for 4 hrs at 65ºC.
8. Centrifuge at 3000 rpm for 5 minutes and wash with PBS.
9. Resuspend pellet in PBS.

10. Extract off lipids using chloroform:methanol:aqueous 8:4:2 keeping the darkly colored, inner phase partition.
11. Add 6M HCl to 10 mL and boil for 1 hr to hydrolyze cellular components.
12. Complete a dialysis against DI water for 14 days at 4°C.
13. Freeze-dry the remaining melanin sample.

3.2 Fungal tissue pyrolysis

Method

1. Sonicate the TMAH for ~45 min. Re-sonicate during inter-sample blanks to keep homogeneous solution.
2. Run 2 blanks on the instrument.
3. Clean the sample tube holders by sonicating in DI water for 1 hour, then rinse with MeOH, soak in MeOH for 15 min and rinse with MeOH and Kim Wipe before use.
4. Weigh out approximately 70 ug of OC into a pyrolysis tube using a tared balance.
5. Using a 10 uL syringe, dispense 15 uL of sonicated TMAH 25% in MeOH into the pyrolysis tube and clean the syringe tip with MeOH and a Kim Wipe to decrease the chances of contaminating the TMAH stock.
6. Run the sample acquisition method, make sure the file will save in a folder with the correct date (YYYYMMDD), and name your sample: Fungal nameHarvest day_Sample replicate_Amount of sample. *For example, a F. avenaceum Sample from harvest day 4, vial 30, with a total sample mass of 0.180 ug would be named FA4_30_180mg.*

7. Affix the pyrolysis tube to a clean sample holder and wipe outside of tube with a Kim Wipe before inserting into the TDU when prompted by the software.
8. When the run is complete, start a blank run, unlock the TDU when prompted, remove the sample holder and tube and insert a clean sample holder without a tube.
9. At the end of the day, clean the syringe with MeOH for 10 rinses.
10. Sample chromatogram (Figure 3.1).

3.3 Cleaning the pyrolysis tubes

1. Recharge NOCHROMIX with new crystals according to directions and let dissolve.
2. Fill shallow glass evaporating dish with NOCHROMIX and py-tubes.
3. With a Pasteur pipette, dispense NOCHROMIX directly into tubes.
4. Let the tubes sit in NOCHROMIX for a total of 24 hours.
5. During the 24 hour period, use the Pasteur pipet to reintroduce the NOCHROMIX into the tubes.
6. Pipette off the NOCHROMIX to be disposed of as waste and thoroughly rinse the tubes with MilliQ water.
7. Soak the tubes in MeOH for 30 min in a covered dish.
8. Transfer the tubes to an ashed beaker and rinse the insides of the tubes with MeOH using a Pasteur pipet. Let sit for 30 min.
9. Rinse the tubes with MeOH.
10. Dry tubes.
11. Transfer tubes to another beaker and ash at 500°C for 4 hours.
12. Quality check at least 10% of the tubes on the Mass Spec (run blank runs).

3.4 Thermochemolysis data analysis

Method

1. Set a 1% threshold of maximal peak area in ChemStation to automatically identify peaks of interest in the total ion chromatogram [TIC].
2. Inspect mass spectrum of each identified peak and compare to library of previously identified compounds. Identify compounds based on spectrum in the library with similar retention times (within 0.2 min) and similar fragmentation patterns after background subtraction.
3. Build a method in MassHunter to detect for the compounds of interest at the proper retention times using only the m/z of interest.
4. Integrate sample files in MassHunter according to the method and then verify peak-by-peak that the retention times are correct and automatic integration captured the peak. If not, choose the appropriate peak or adjust the integration in order to capture the whole peak.
5. Export the data into Excel and manually delete any integrations that were not identified as peaks of interest in the TIC.
    a. Where replicates have been run, keep only peaks that are identified in 2 of the 3 replicate samples in order to avoid analysis of contaminates or ghost peaks.
6. Divide the area count of the integrated peak by the sample weight loaded and ratio organic carbon in the sample.

$$\frac{\text{Area count}}{(\text{sample weight,g} * \text{ratio organic carbon})} = \text{Area count}_{\text{OC normalized}} \quad \text{(Eq 5)}$$

7. Divide the OC normalized peak area by the sum of all the OC normalized peaks to get a ratio of how much this single peak contributed to the whole sample response.

$$\frac{\text{Area Count}_{\text{OC normalized}}}{\sum(\text{Area Count}_{\text{OC normalized,i}})} = \text{Peak Contribution} \quad \text{(Eq 6)}$$

8. To represent how much of each compound class is present in the sample, take the sum of the single peak contributions across the compound class.

$\sum(\text{Peak Contribution}_{\text{h}}) = \text{Compound Class Contribution}_{\text{h}}$, where h = aromatic, sugar, lipid, sterol, n-containing, or unspecified (Eq 7)

9. Where replicates have been run, calculate the variance of each peaks Peak Contribution.

$$\frac{\text{Peak Contribution} - \text{Peak Contribution}_{\text{Average}}}{\text{n}-1} = \sigma_{\text{Peak}} \quad \text{(Eq 8)}$$

10. Compound the error across the compound class by taking the square root of the sum of the variance of peaks contributing to the compound class.

$\sqrt{\sum \sigma_{\text{peak}}}$ = Error of Compound Class (Eq 9)

3.5 Standard Addition

A standard addition calibration experiment was completed with *F. avenaceum* and spiked in standard material. Standards used included mannan (isolated from *Saccharomyces cerevisiae* via alkaline extraction, Sigma), chitin (isolated from shrimp shells, Sigma) and ergosterol (USP certified reference grade, Sigma). A differing amount of standard was added to four samples of lyophilized fungal tissue and then each was processed with a ball mill grinder for complete homogenization. The samples were then

placed in a desiccator for 1 week before use. Thermochemolysis-GCMS was carried out on this tissue under the same conditions as described in Chapter 2. Figure 3.2 describes the results of this test where the total sugar or total sterol response is shown to increase with amount of corresponding standard added to the sample loaded onto column.

3.6 Kinetics data treatment

Single G Model

The single G model is based on simple first order kinetic consumption of organic carbon [G]. This model states that the rate of consumption of G is directly proportional to the rate constant k and the concentration of G.

$$\frac{-dG}{dt} = k\,G \qquad \text{(Eq 10)}$$

Equation 10 is rearranged and integrated to yield

$$\ln\left(\frac{G_t}{G_0}\right) = -kt \qquad \text{(Eq 11)}$$

Here, we take the natural logarithm of normalized carbon mass (carbon mass at time t (G_t), normalized to the initial mass (G_0)). This logarithm displays a dependence on the time variable that is scaled by the kinetic rate constant k.

An exponential expression derived from Equation 11 is also used to fit the data.

$$\frac{G_t}{G_0} = e^{-kt} \qquad \text{(Eq 12)}$$

Equation 12 has the advantage of not transforming the original data set outside of normalizing it to the original mass. Because transformed data also has transformed error

margins, some consider transforming original data sets to be problematic as a way to fit data. The exponential fit from Equation 12 has been used in Chapter 2 for all species.

Double G Model

An extension of the Single G model, termed the multi-G model uses the same simple understanding of first order kinetics and expands upon it to describe more than one pool of degrading carbon. A 2-pool model, or Double G model, was employed here. Carbon pool 1 or G_1 is controlled by kinetic constant k_1 and is a fast degrading pool. This is thought to be the carbon of the decaying matter that is most accessible to enzymatic degradation or is most energetically desirable for metabolism by microorganisms. Once carbon pool 1 is mostly or completely degraded away, the rate of the total carbon degradation slows according to the more difficult to degrade carbon that is left. This remaining carbon, G_2, belongs to carbon pool 2 and is controlled by a slower kinetic rate, k_2. The degradation of pool 1 and pool 2 happen in parallel and both contribute to the rate of the overall carbon loss. Equation 10 is the basis of this model but the integration of this can be expressed in a more detailed way as shown below in Equation 13.

$$\ln\left(\frac{G_t}{G_0}\right) = -f(k)t \qquad \text{(Eq 13)}$$

Here, f(k) refers to how the rate constant k is no longer represented by a single value and is instead a function of the carbon pool. Since in the double G model, there are two distinct carbon pools, the right-hand side of the equation can be expressed more fully as the sum of the two k values.

$$\ln\left(\frac{G_t}{G_0}\right) = -k_1 t - k_2 t \qquad \text{(Eq 14)}$$

Here again, Equation 14 has the log of the relative mass values being dependent on the product of time and a kinetic constant.

In order to allow more degrees of freedom in the fit parameters, an equivalent biexponential model was fit to the total data set. This model eliminates the discontinuity involved in the fit of the logarithm of the relative mass which has to be decided by hand in the discontinuous, linear model and could introduce bias. The biexponential model describes the first order kinetic decays of pool 1 and pool 2 contributing a weighted portion to the overall decay function.

$$\frac{G_t}{G_0} = \beta_{1,0} e^{-k_1 t} + \beta_{2,0}\, e^{-k_2 t} \qquad \text{(Eq 15)}$$

In Equation 15, $\beta_{1,0}$ and $\beta_{2,0}$ describe what percentage of the total carbon existed in each pool at time 0. These two variables can be considered as weighting parameters to divide up the behavior of G_t as attributed to the first exponential and to the second exponential. In optimizing this model, the proportion of G within each carbon pool was determined by looking at a histogram of rate values for each data set. The rate would be the difference in material over the difference in time for each separate data point. Each rate value should then represent the average rate value over the days in which it occurred. In other words, the fast kinetic that appears between day 1 and 2 should represent one frequency value of rate whereas the slow kinetic observed between day 14 and day 28 should represent 14 days over which the average rate is represented by the calculated rate value.

From the frequency distribution of the data, the ratio of material in each carbon pool was fixed ($1- \beta_{1,0}= \beta_{2,0}$) and the double G exponential was fit to develop the first estimates for the value of k_1 and k_2. These estimates were then plugged in to the model

again and the value of $\beta_{1,0}$ was allowed to be fit (1- $\beta_{1,0}$= $\beta_{2,0}$). This consecutive fit pattern occurred four times with the standard error changing only on the order of the thousanths place. The exponential fit is perferred over the linear fit as it is based on the raw data. The exponential fit of Equation 15 was used to find kinetic parameters for all species as reported in chapter 2. Final fits of this data are represented in Figure 3.3.

Tables

Table 2.1: Degradation properties for mass loss of studied fungi. A single (Single G) or biexponential (Double G) function was fit to the data of a 28-day degradation sequence for *Xylaria*, *Hydnotrya*, and *Ascomycota*. *F. avenaceum* data was fit over 21 days.

Species	Ratio Mass Remaining	Single G Model		Double G Model					
		k, day^{-1}	turnover, day	G_1	k_1, day^{-1}	$turnover_1$, day	G_2	k_2, day^{-1}	$turnover_2$, day
Xylaria	0.252	0.167	5.99	0.739	0.299	3.34	0.261	0.02124	47.1
Hydnotrya	0.483	0.0503	19.9	-	-	-	-	-	-
Ascomycota	0.120	0.127	7.87	0.801	0.171	5.85	0.199	0.03033	33.0
F. avenaceum	0.308	0.139	7.19	0.720	0.297	3.37	0.280	0.00899	111

* Day 28 was disregarded for the fit of *F. avenaceum* tissue.

Table 2.2: Degradation kinetic properties for elemental losses of studied fungi. A single G modle function was fit to the data for each species over the 28 day series except for *Hydnotrya.* Day 28 was disregarded for the fit of *F. avenaceum* tissue.

Species	Carbon Single G Model		Nitrogen Single G Model	
	k, day^{-1}	turnover, day	k_1, day^{-1}	$turnover_1$, day
Xylaria	0.0178	56.18	0.27	3.70
Hydnotrya	-	-	-	-
Ascomycota	0.0285	35.09	0.0358	27.93
F. avenaceum	0.0212	47.17	0.0308	32.47

Table 2.3: Carbon and nitrogen values across the study period.

Species	Harvest Day	Nitrogen Day 0:Harvest (wt%)	Carbon Day 0:Harvest (wt%)	C:N (atomic)
F. avenaceum	0	1	1	7.280
	1	1.005	1.117	8.091
	2	0.885	1.074	8.838
	4	0.920	1.018	8.139
	7	0.630	0.704	8.139
	14	0.555	0.643	8.436
	21	0.433	0.518	8.705
	28	0.658	0.741	8.078
Hydnotrya	0	1	1	8.729
	1	0.951	0.971	8.734
	2	0.977	0.985	8.629
	7	0.882	0.903	8.701
	28	1.047	0.912	7.472
Xylaria	0	1	1	8.198
	1	0.785	0.995	10.405
	2	0.746	0.994	10.942
	4	0.747	0.959	10.583
	7	0.720	0.919	10.473
	14	0.609	0.630	8.436
	28	0.656	0.680	8.316
Ascomyota	0	1	1	6.137
	1	0.866	0.938	6.623
	2	0.882	0.980	6.782
	4	0.726	0.908	7.638
	7	0.684	0.770	6.890
	14	0.590	0.594	6.140
	28	0.496	0.523	6.406

Table 2.4: Ratio of category peak area to total peak area for all species. Peaks are assigned to only one category. The lipids category contains only non-sterol lipids and any compound with nitrogen was assigned to the n-containing category.

		Aromatic	Lipid	N-containing	Sterol	Sugar	Unspecified
Species	Harvest Day	Compound:Total	Compound:Total	Compound:Total	Compound:Total	Compound:Total	Compound:Total
F. avenaceum	0	4.20	18.03	35.77	0.79	33.64	7.55
	1	4.08	38.72	16.87	0.15	35.43	4.75
	2	9.30	29.31	11.22	1.01	37.72	11.44
	4	5.10	33.33	11.57	2.77	36.24	10.98
	7	9.03	25.29	15.46	0.88	30.14	19.20
	21	9.55	37.07	5.23	8.17	29.58	10.40
	28	5.90	23.57	9.01	11.50	35.41	14.62
Hydnotrya	0	31.26	31.07	6.81	0.63	28.10	2.14
	1	8.78	36.24	18.31	2.92	29.77	3.97
	7	6.01	24.11	14.29	4.02	46.79	4.77
	28	3.22	20.42	35.90	11.96	20.44	8.06
Xylaria	0	9.56	25.20	9.61	0.67	48.84	6.13
	1	6.03	25.60	8.49	0.41	49.26	10.21
	2	7.86	33.27	0.00	0.44	46.60	11.83
	4	11.16	15.19	8.19	0.86	47.75	16.85
	7	7.69	28.20	3.10	2.20	49.97	8.85
	14	10.65	14.93	4.60	3.51	55.05	11.26
	28	8.36	17.64	3.70	1.84	55.81	12.65
Ascomyota	0	3.24	63.50	4.78	1.86	26.08	0.55
	1	10.28	58.86	4.32	0.41	15.74	10.39
	2	5.51	55.61	3.21	1.09	24.97	5.75
	7	5.27	53.44	5.21	3.24	27.97	4.87
	14	6.99	52.32	8.91	5.21	17.06	9.52
	28	9.82	28.12	8.15	4.84	37.13	11.94

Figures

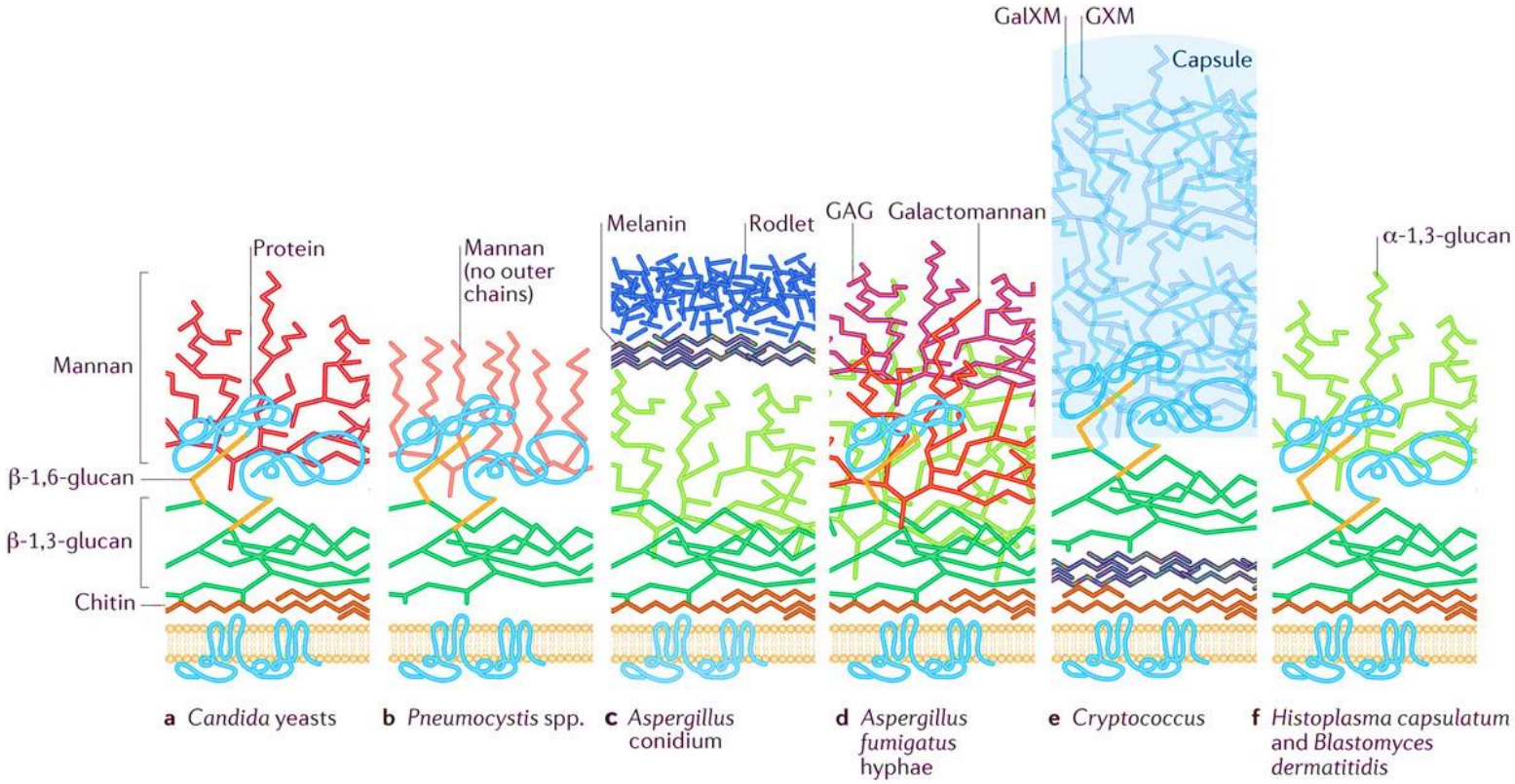

Figure 1.1: Fungal cell wall organization across different species (Erwig and Gow, 2016).

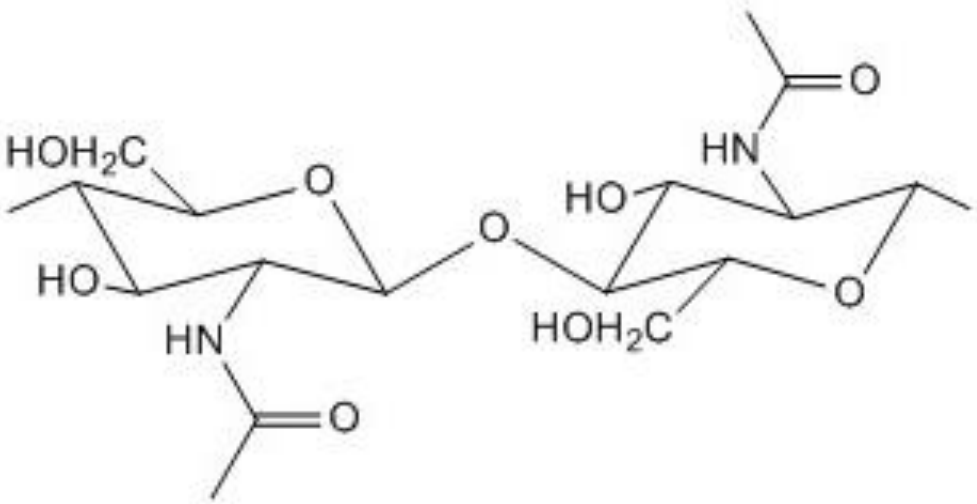

Figure 1.2: *N*-acetylglucosamine. Linked in a β (1→4) bond as in the chitin polymer.

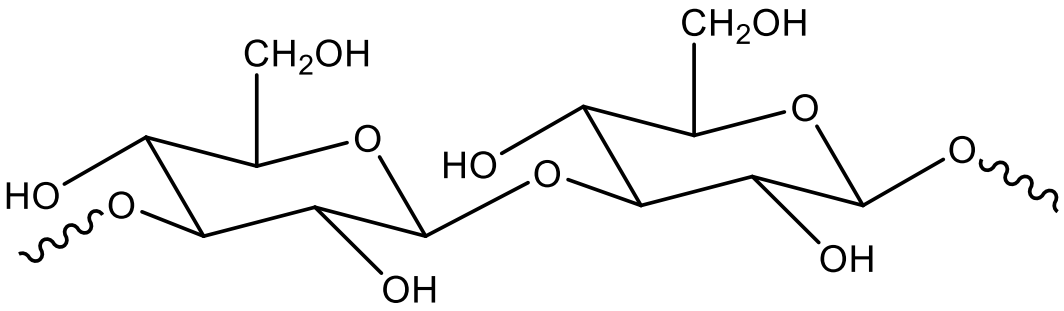

Figure 1.3: β(1-3) linked glucose monomers.

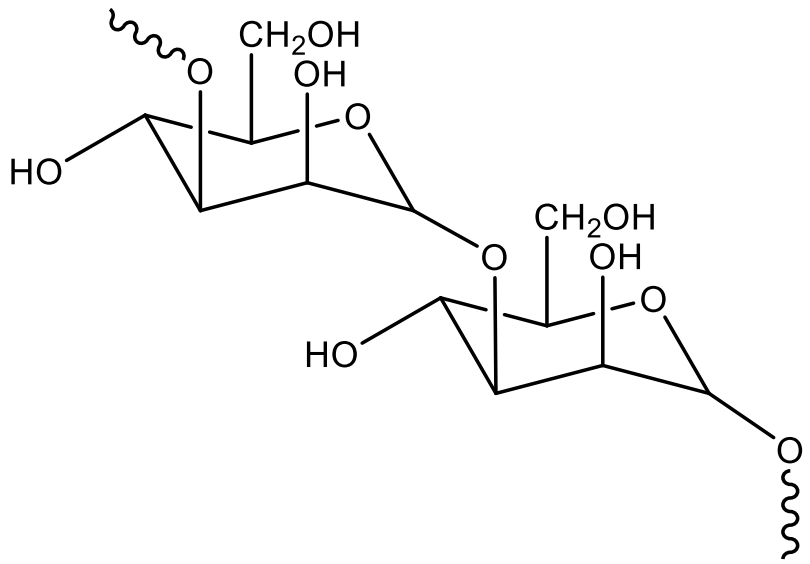

Figure 1.4: α(1-6) linked mannose monomers.

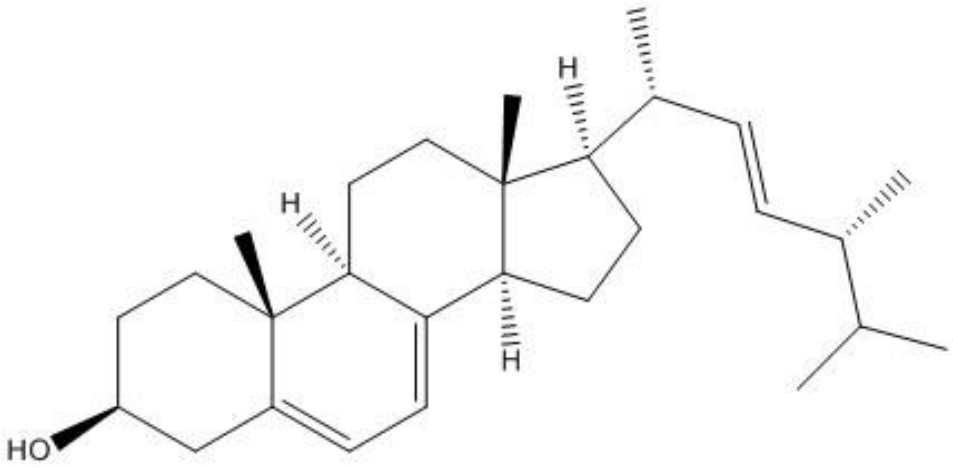

Figure 1.5: Ergosterol membrane sterol.

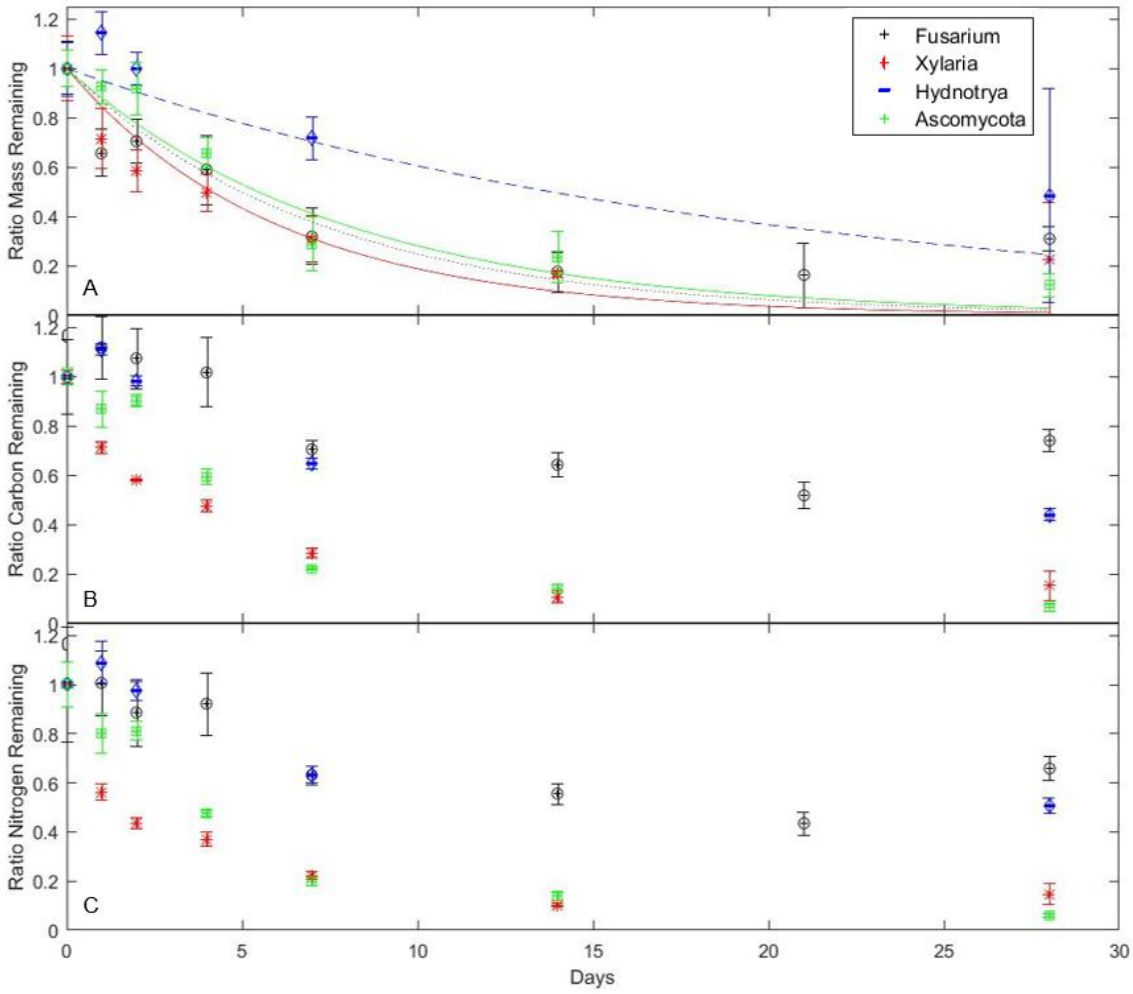

Figure 2.1: Bulk degradation properties of studied fungi. Data on each graph represents a ratio of the total mass (a), organic carbon weight (b), or nitrogen weight (c) that was recovered on each harvest day over the day zero weight. Error bars represent the standard deviation from field replicates. The trend lines in (a) correspond to the single order exponential fit of the total mass data.

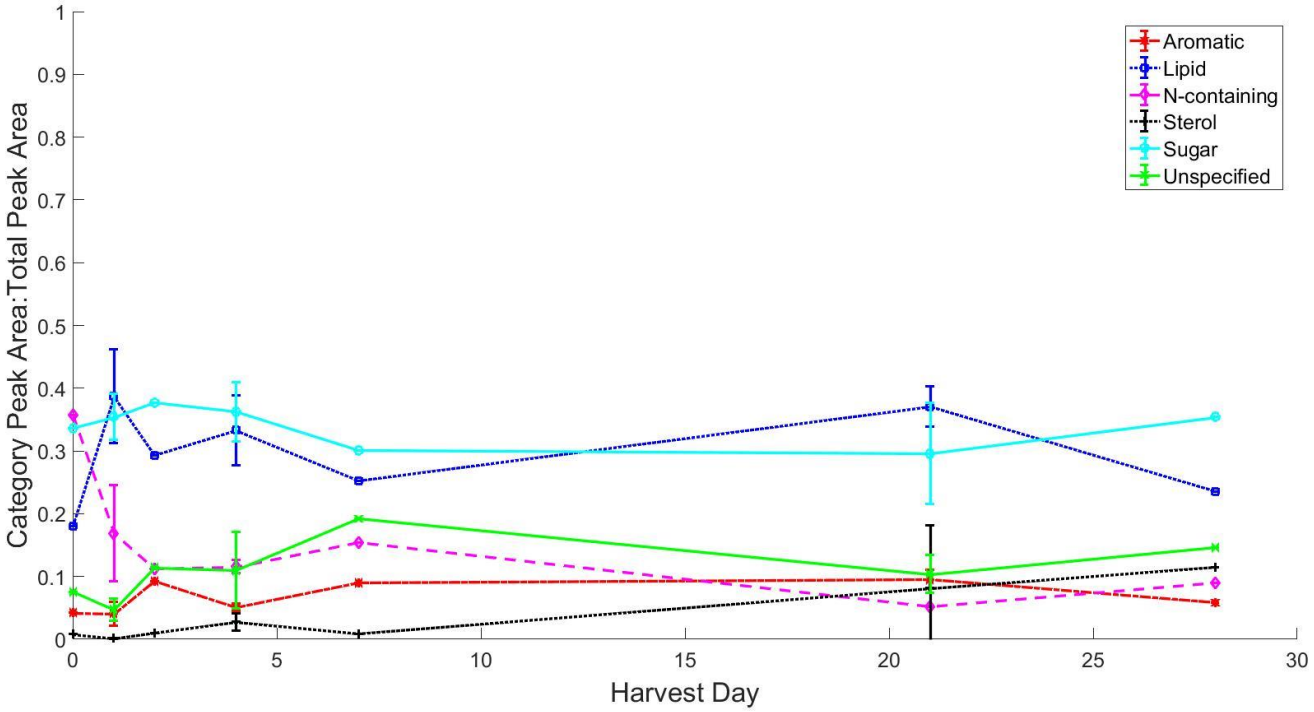

Figure 2.2: Chemical degradation of *F. avenaceum* tissue. Data represents fractional composition of the total tissue at each harvest day according to aromatic, lipid, N-containing, sterol, sugar, and unspecified compounds as determined by TMAH py-GCMS. Error bars represent the propagated standard deviation of each category of peaks for three different field replicates.

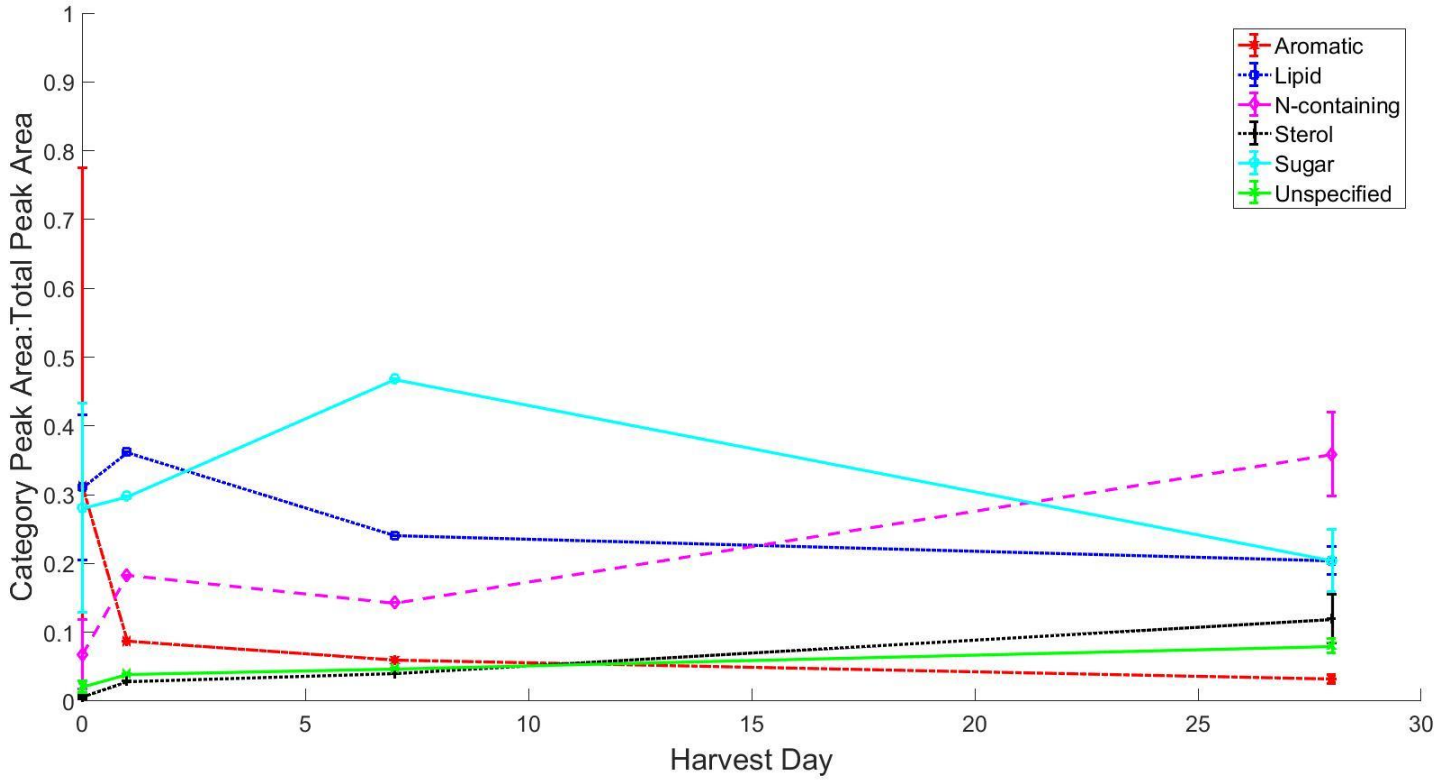

Figure 2.3: Chemical degradation of *Hydnotrya* tissue. Data represents fractional composition of the total tissue at each harvest day according to aromatic, lipid, N-containing, sterol, sugar, and unspecified compounds as determined by TMAH py-GCMS. Error bars represent the propagated standard deviation of each category of peaks for three different field replicates.

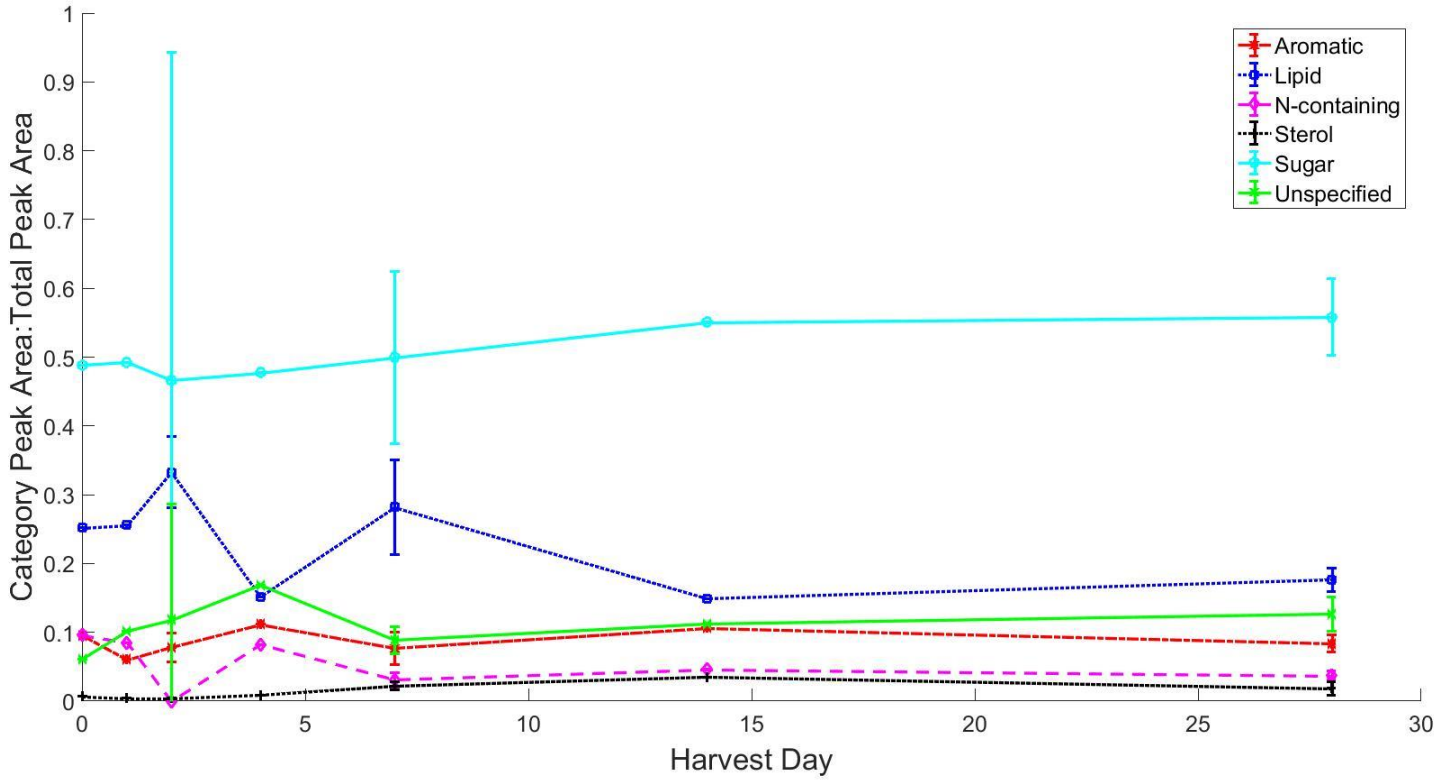

Figure 2.4: Chemical degradation of *Xylaria* tissue. Data represents fractional composition of the total tissue at each harvest day according to aromatic, lipid, N-containing, sterol, sugar, and unspecified compounds as determined by TMAH py-GCMS. Error bars represent the propagated standard deviation of each category of peaks for three different field replicates.

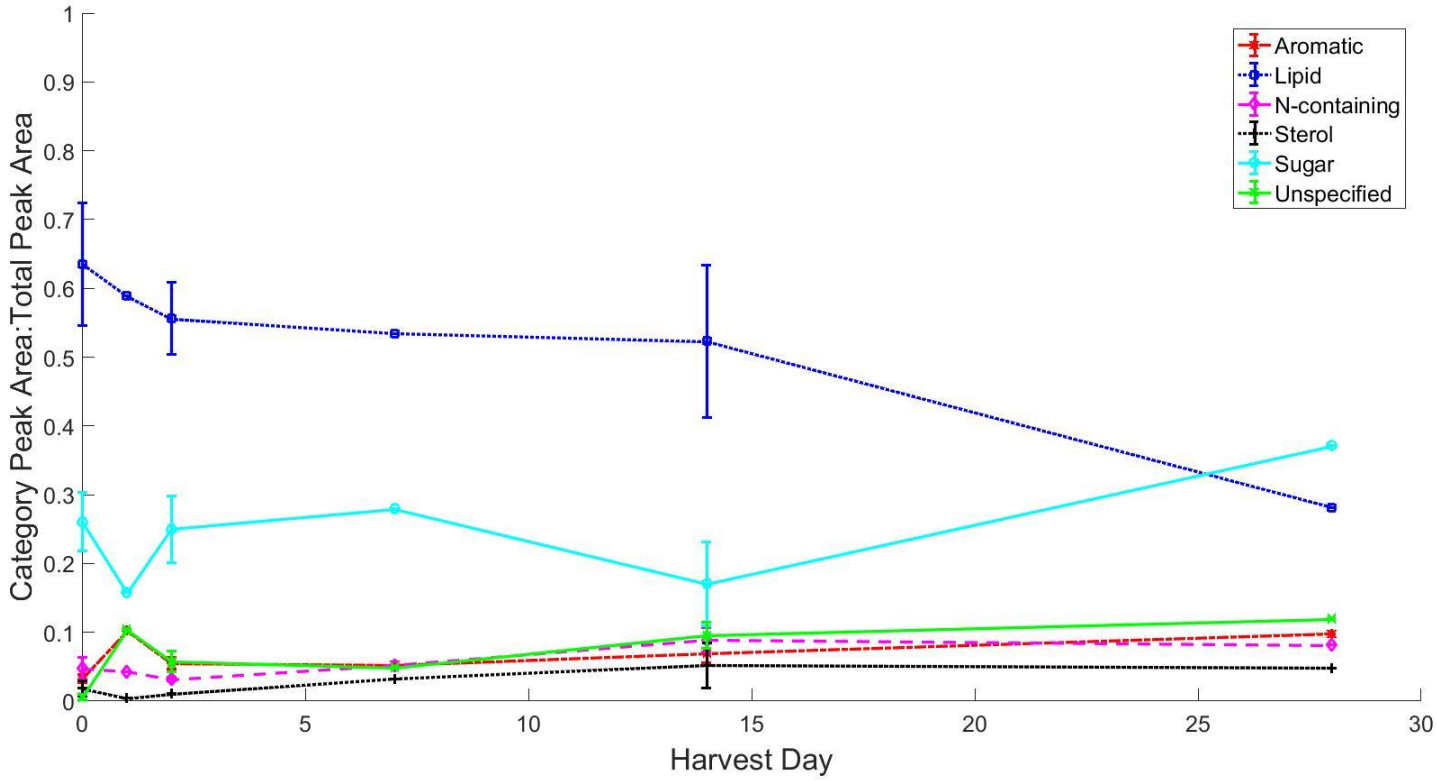

Figure 2.5: Chemical degradation of the *Ascomycota* tissue. Data represents fractional composition of the total tissue at each harvest day according to aromatic, lipid, N-containing, sterol, sugar, and unspecified compounds as determined by TMAH py-GCMS. Error bars represent the propagated standard deviation of each category of peaks for three different field replicates.

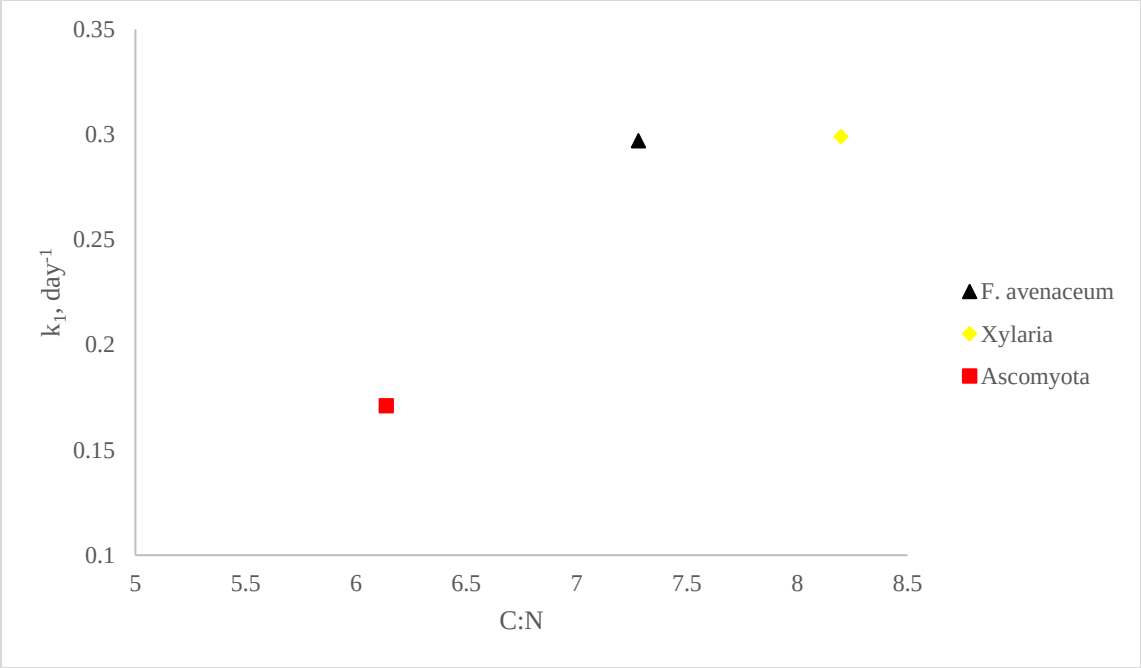

Figure 2.6: Initial kinetics and C:N ratio of tissues. Double G kinetic constant k_1 is related to the initial, Day 0, atomic C:N ratio of the tissues. *Hydnotrya* was not fit with the double G model due to decreased sample density.

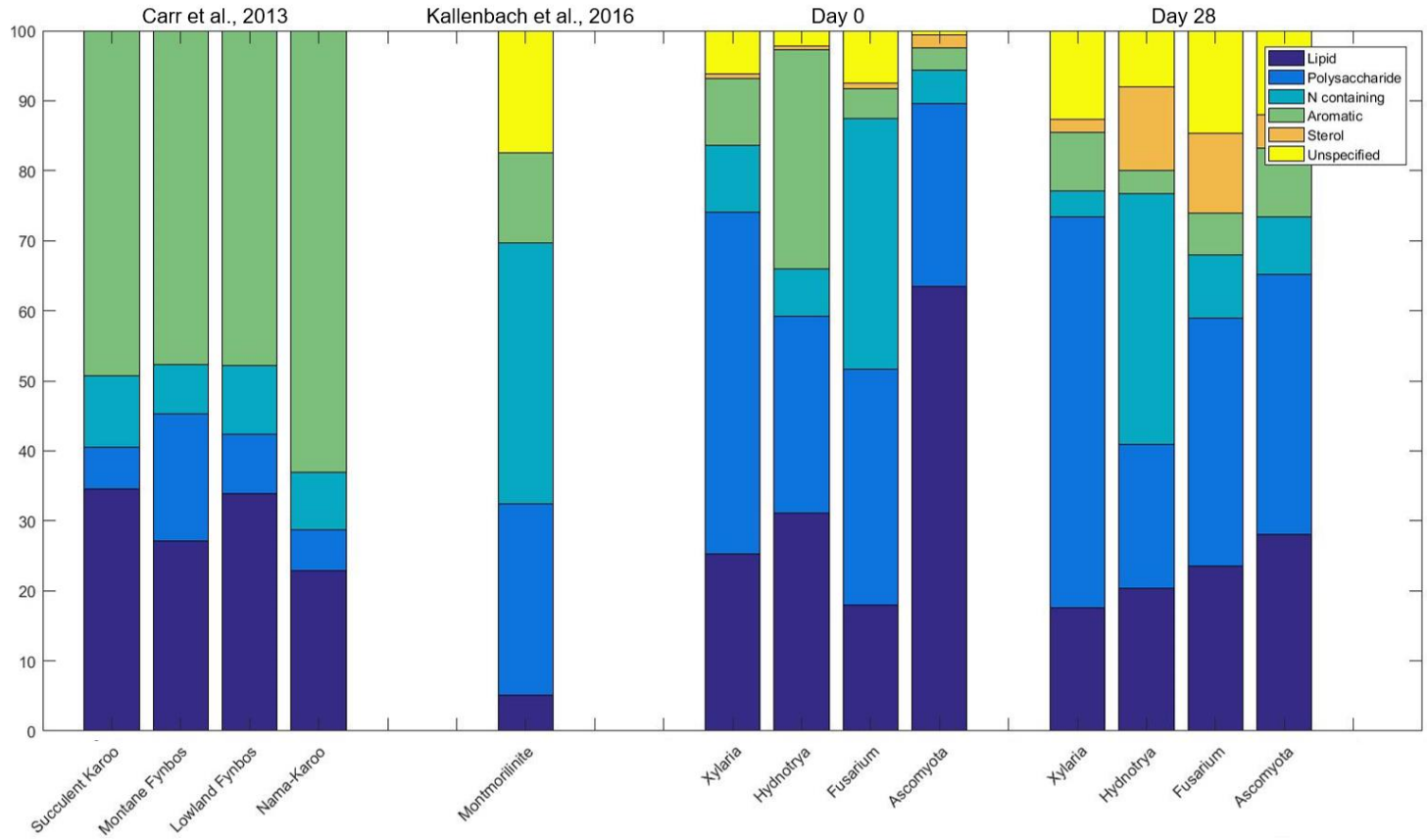

Figure 2.7: Chemical makeup of natural soils compared to fungal tissue. Natural soils from different environments as presented by Carr et al, 2013 and Kallenbach et al., 2016 along with chemical composition of the fungal tissue on day 0 and day 28.

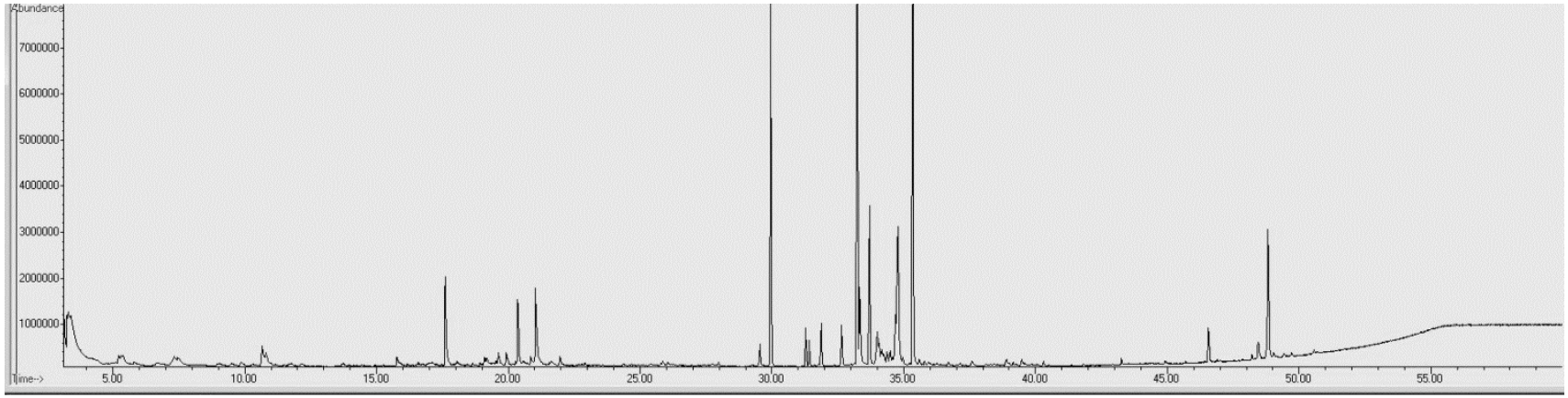

Figure 3.1: Sample total ion chromatogram. *Hydnotrya*.day 0 chromatogram.

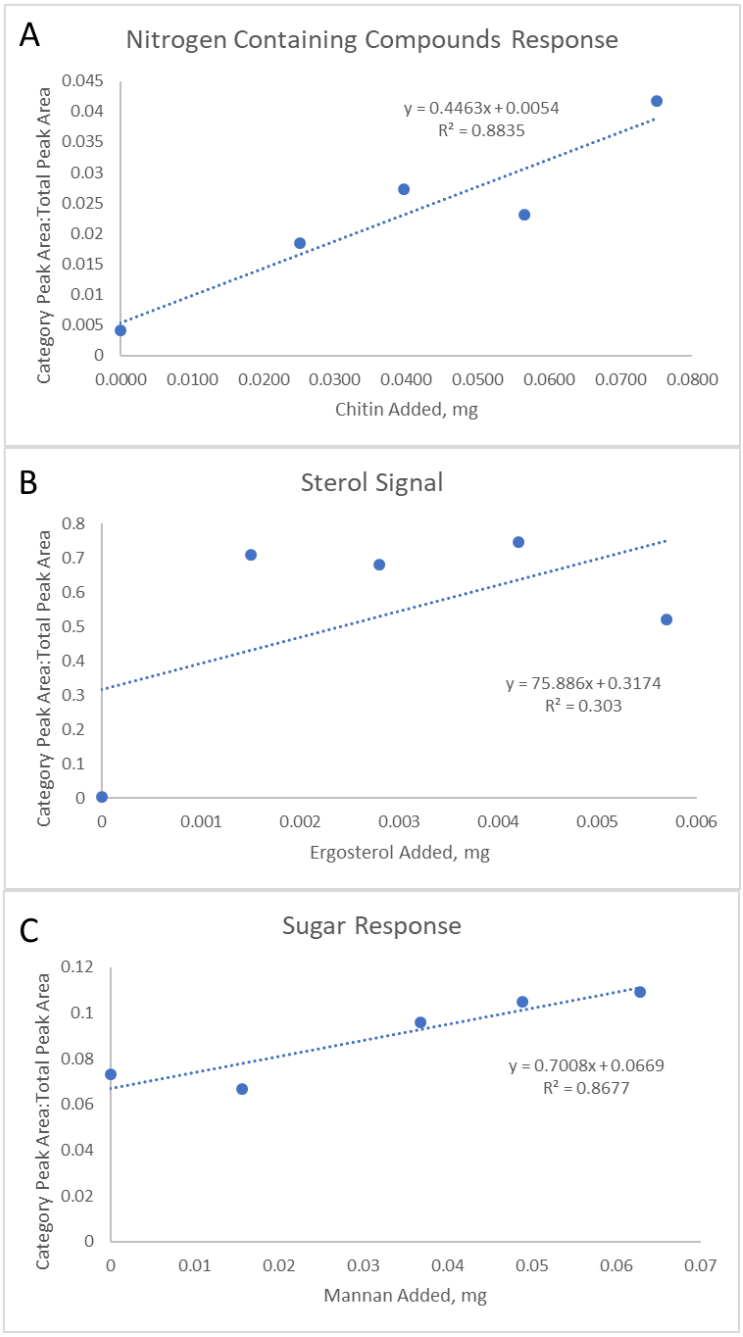

Figure 3.2: Standard addition calibration test. *F. avenaceum* was spiked with chitin (A), ergosterol (B), and mannan (C) for thermochemolysis py-GCMS analysis.

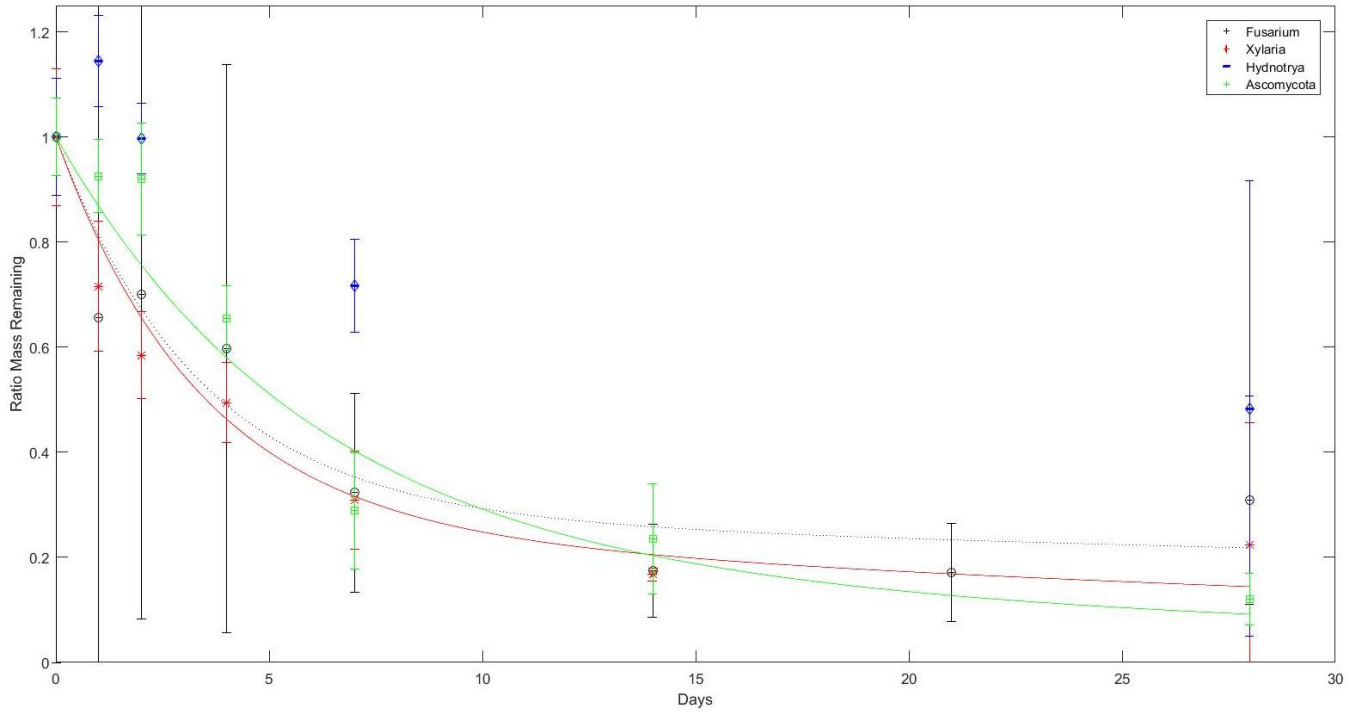

Figure 3.3: Degradation properties of studied fungi via Double G kinetics. Data represents normailzed bulk mass for each studied species and corresponding fit lines are the results of iterative Double G fitting procedures using R. Error bars represent the standard deviation from field replicates.

WORKS CITED

Adamczyk, Bartosz, Outi Maaria Sietiö, Christina Biasi, and Jussi Heinonsalo. 2019. "Interaction between Tannins and Fungal Necromass Stabilizes Fungal Residues in Boreal Forest Soils." *New Phytologist* 223(1).

Aguilar-Uscanga, B., and J. M. Francois. 2003. "A Study of the Yeast Cell Wall Composition and Structure in Response to Growth Conditions and Mode of Cultivation." *Letters in Applied Microbiology* 37(3):268–74. doi: 10.1046/j.1472-765x.2003.01394.x.

Ahrazem, Oussama, Alicia Prieto, Juan Antonio Leal, Begoña Gómez-Miranda, Jezabel Domenech, Jesús Jiménez-Barbero, and Manuel Bernabé. 1997. "Structural Elucidation of Acidic Fungal Polysaccharides Isolated from the Cell-Wall of Genera Cylindrocladium and Calonectria." *Carbohydrate Research* 303(1):67–72. doi: 10.1016/s0008-6215(97)00145-6.

Baldrian, Petr, Jana Voříšková, Petra Dobiášová, Věra Merhautová, Ludmila Lisá, and Vendula Valášková. 2010. "Production of Extracellular Enzymes and Degradation of Biopolymers by Saprotrophic Microfungi from the Upper Layers of Forest Soil." *Plant and Soil* 338(1–2):111–25. doi: 10.1007/s11104-010-0324-3.

Bergmann, Werner, and John A. Klacsmann. 1948. "Ergosterol F1." *The Journal of Organic Chemistry* 13(1):21–25. doi: 10.1021/jo01159a003.

Berner, Robert A. 1964. "An Idealized Model of Dissolved Sulfate Distribution in Recent Sediments." *Geochimica et Cosmochimica Acta* 28(9):1497–1503. doi: 10.1016/0016-7037(64)90164-4.

Bernhardt, Emily, and William Schlesinger. 2013. *Biogeochemistry: An Analysis of Global Change*. 3rd ed. Elsevier.

Betts, Richard A., Peter D. Falloon, Kees Klein Goldewijk, and Navin Ramankutty. 2007. "Biogeophysical Effects of Land Use on Climate: Model Simulations of Radiative Forcing and Large-Scale Temperature Change." *Agricultural and Forest Meteorology* 142(2–4). doi: 10.1016/j.agrformet.2006.08.021.

Blagodatsky, Sergey, and Pete Smith. 2012. "Soil Physics Meets Soil Biology: Towards Better Mechanistic Prediction of Greenhouse Gas Emissions from Soil." *Soil Biology and Biochemistry* 47:78–92. doi: 10.1016/j.soilbio.2011.12.015.

Bontti, Eliana E., Joseph P. Decant, Seth M. Munson, Mark A. Gathany, Agnieszka Przeszlowska, Michelle L. Haddix, Stephanie Owens, Ingrid C. Burke, WIlliam J. Parton, and Mark E. Harmon. 2009. "Litter Decomposition in Grasslands of Central North America (US Great Plains)." *Global Change Biology* 15(5):1356–63. doi: 10.1111/j.1365-2486.2008.01815.x.

Bossuyt, H., K. Denef, J. Six, S. D. Frey, R. Merckx, and K. Paustian. 2001. "Influence of Microbial Populations and Residue Quality on Aggregate Stability." *Applied Soil Ecology* 16(3):195–208. doi: 10.1016/s0929-1393(00)00116-5.

Brown, Margaret E., and Michelle C. Y. Chang. 2014. "Exploring Bacterial Lignin Degradation." *Current Opinion in Chemical Biology* 19:1–7. doi: 10.1016/j.cbpa.2013.11.015.

Bryant, David M., Elisabeth A. Holland, Timothy R. Seastedt, and Marilyn D. Walker. 1998. "Analysis of Litter Decomposition in an Alpine Tundra." *Canadian Journal of*

Botany 76(7):1295–1304. doi: 10.1139/b98-117.

Burges, N. A., H. M. Hurst, and Beryl Walkden. 1964. "The Phenolic Constituents of Humic Acid and Their Relation to the Lignin of the Plant Cover." *Geochimica et Cosmochimica Acta* 28(10):1547–54. doi: https://doi.org/10.1016/0016-7037(64)90005-5.

Butler, M. J., and A. W. Day. 1998. "Fungal Melanins: A Review." *Canadian Journal of Microbiology* 44(12):1115–36. doi: 10.1139/cjm-44-12-1115.

Calderón, Francisco J., Gregory W. McCarty, and James B. Reeves. 2006. "Pyrolisis-MS and FT-IR Analysis of Fresh and Decomposed Dairy Manure." *Journal of Analytical and Applied Pyrolysis* 76(1–2). doi: 10.1016/j.jaap.2005.06.009.

Campbell, Eleanor E., and Keith Paustian. 2015. "Current Developments in Soil Organic Matter Modeling and the Expansion of Model Applications: A Review." *Environmental Research Letters* 10(12).

Carr, Andrew S., Arnoud Boom, Brian M. Chase, Michael E. Meadows, Zoë E. Roberts, Matthew N. Britton, and Alex M. J. Cumming. 2013. "Biome-Scale Characterisation and Differentiation of Semi-Arid and Arid Zone Soil Organic Matter Compositions Using Pyrolysis–GC/MS Analysis." *Geoderma* 200–201:189–201. doi: https://doi.org/10.1016/j.geoderma.2013.02.012.

Casadevall, Arturo, Antonio Nakouzi, Pier R. Crippa, and Melvin Eisner. 2012. "Fungal Melanins Differ in Planar Stacking Distances." *PLoS ONE* 7(2):e30299. doi: 10.1371/journal.pone.0030299.

Celi, Luisella, Morris Schnitzer, and Michèle Nègre. 1997. "Analysis of Carboxyl Groups

in Soil Humic Acids by a Wet Chemical Method, Fourier-Transform Infrared Spectrophotometry, and Solution-State Carbon-13 Nuclear Magnetic Resonance. A Comparative Study." *Soil Science* 162(3):189–97. doi: 10.1097/00010694-199703000-00004.

Certano, Amanda K., Christopher W. Fernandez, Katherine A. Heckman, and Peter G. Kennedy. 2018. "The Afterlife Effects of Fungal Morphology: Contrasting Decomposition Rates between Diffuse and Rhizomorphic Necromass." *Soil Biology and Biochemistry* 126. doi: 10.1016/j.soilbio.2018.08.002.

Challinor, J. M. 1995. "Characterisation of Wood by Pyrolysis Derivatisation—Gas Chromatography/Mass Spectrometry." *Journal of Analytical and Applied Pyrolysis* 35(1):93–107. doi: 10.1016/0165-2370(95)00903-r.

Challinor, John M. 2001. "Review: The Development and Applications of Thermally Assisted Hydrolysis and Methylation Reactions." *Journal of Analytical and Applied Pyrolysis* 61(1–2):3–34. doi: 10.1016/s0165-2370(01)00146-2.

Coleman, K., and D. S. Jenkinson. 1996. "RothC-26.3 - A Model for the Turnover of Carbon in Soil BT - Evaluation of Soil Organic Matter Models." Pp. 237–46 in, edited by D. S. Powlson, P. Smith, and J. U. Smith. Berlin, Heidelberg: Springer Berlin Heidelberg.

Cong, Rihuan, Xiujun Wang, Minggang Xu, Stephen M. Ogle, and William J. Parton. 2014. "Evaluation of the CENTURY Model Using Long-Term Fertilization Trials under Corn-Wheat Cropping Systems in the Typical Croplands of China." *PLoS ONE* 9(4). doi: 10.1371/journal.pone.0095142.

Cornish-Bowden, A. 1999. *Basic Mathematics for Biochemists*. Oxford University Press.

Cotrufo, M. Francesca, Phil Ineson, and J. Derek Roberts. 1995. "Decomposition of Birch Leaf Litters with Varying C-to-N Ratios." *Soil Biology and Biochemistry* 27(9):1219–21. doi: 10.1016/0038-0717(95)00043-e.

Cotton, Jon, and Veronica Acosta-Martínez. 2018. "Intensive Tillage Converting Grassland to Cropland Immediately Reduces Soil Microbial Community Size and Organic Carbon." *Agricultural & Environmental Letters* 3(1). doi: 10.2134/ael2018.09.0047.

Dornbush, Mathew, Cynthia Cambardella, Elaine Ingham, and James Raich. 2008. "A Comparison of Soil Food Webs beneath C3- and C 4-Dominated Grasslands." *Biology and Fertility of Soils* 45(1). doi: 10.1007/s00374-008-0312-4.

Drigo, B., I. C. Anderson, G. S. K. Kannangara, J. W. G. Cairney, and D. Johnson. 2012. "Rapid Incorporation of Carbon from Ectomycorrhizal Mycelial Necromass into Soil Fungal Communities." *Soil Biology and Biochemistry* 49:4–10. doi: 10.1016/j.soilbio.2012.02.003.

Duboc, Ph, N. Schill, L. Menoud, W. Van Gulik, and U. Von Stockar. 1995. "Measurements of Sulfur, Phosphorus and Other Ions in Microbial Biomass: Influence on Correct Determination of Elemental Composition and Degree of Reduction." *Journal of Biotechnology* 43(2). doi: 10.1016/0168-1656(95)00135-0.

Dworzanski, Jacek P., Luc Berwald, William H. McClennen, and Henk L. C. Meuzelaar. 1991. "Mechanistic Aspects of the Pyrolytic Methylation and Transesterification of Bacterial Cell Wall Lipids." *Journal of Analytical and Applied Pyrolysis* 21(1–

2):221–32. doi: 10.1016/0165-2370(91)80027-6.

Eisenman, Helene C., and Arturo Casadevall. 2011. “Synthesis and Assembly of Fungal Melanin.” *Applied Microbiology and Biotechnology* 93(3):931–40. doi: 10.1007/s00253-011-3777-2.

Eisenman, Helene C., Joshua D. Nosanchuk, J. Beau W. Webber, Ray J. Emerson, Terri A. Camesano, and Arturo Casadevall. 2005. “Microstructure of Cell Wall-Associated Melanin in the Human Pathogenic FungusCryptococcus Neoformans†.” *Biochemistry* 44(10):3683–93. doi: 10.1021/bi047731m.

Enochs, W. S., M. J. Nilges, and H. M. Swartz. 1993. “A Standardized Test for the Identification and Characterization of Melanins Using Electron Paramagnetic Resonance (EPR) Spectroscopy.” *Pigment Cell Research* 6(2):91–99. doi: 10.1111/j.1600-0749.1993.tb00587.x.

Fabbri, D., and R. Helleur. 1999. “Characterization of the Tetramethylammonium Hydroxide Thermochemolysis Products of Carbohydrates.” *Journal of Analytical and Applied Pyrolysis* 49(1–2):277–93. doi: 10.1016/s0165-2370(98)00085-0.

Fernandez, Christopher W., Katherine Heckman, Randall Kolka, and Peter G. Kennedy. 2019. “Melanin Mitigates the Accelerated Decay of Mycorrhizal Necromass with Peatland Warming.” *Ecology Letters* 22(3).

Fernandez, Christopher W., and Roger T. Koide. 2012. “The Role of Chitin in the Decomposition of Ectomycorrhizal Fungal Litter.” *Ecology* 93(1):24–28. doi: 10.1890/11-1346.1.

Fernandez, Christopher W., and Roger T. Koide. 2013. “The Function of Melanin in the

Ectomycorrhizal Fungus Cenococcum Geophilum under Water Stress." *Fungal Ecology* 6(6):479–86. doi: 10.1016/j.funeco.2013.08.004.

Fernandez, Christopher W., and Roger T. Koide. 2014. "Initial Melanin and Nitrogen Concentrations Control the Decomposition of Ectomycorrhizal Fungal Litter." *Soil Biology and Biochemistry* 77:150–57. doi: 10.1016/j.soilbio.2014.06.026.

Flaig, W. 1964. "Effects of Micro-Organisms in the Transformation of Lignin to Humic Substances." *Geochimica et Cosmochimica Acta* 28(10):1523–35. doi: https://doi.org/10.1016/0016-7037(64)90003-1.

Fogel, Robert, and Kermit Cromack Jr. 1977. "Effect of Habitat and Substrate Quality on Douglas Fir Litter Decomposition in Western Oregon." *Canadian Journal of Botany* 55(12):1632–40. doi: 10.1139/b77-190.

Follett, Ronald F., Eldor A. Paul, and Elizabeth G. Pruessner. 2007. "Soil Carbon Dynamics during a Long-Term Incubation Study Involving 13C and 14C Measurements." *Soil Science* 172(3):189–208. doi: 10.1097/ss.0b013e31803403de.

Francois, Jean Marie. 2007. "A Simple Method for Quantitative Determination of Polysaccharides in Fungal Cell Walls." *Nature Protocols* 1(6):2995–3000. doi: 10.1038/nprot.2006.457.

Frey, S. D., R. Drijber, H. Smith, and J. Melillo. 2008. "Microbial Biomass, Functional Capacity, and Community Structure after 12 Years of Soil Warming." *Soil Biology and Biochemistry* 40(11). doi: 10.1016/j.soilbio.2008.07.020.

Frey, S. D., E. T. Elliott, and K. Paustian. 1999. "Bacterial and Fungal Abundance and Biomass in Conventional and No-Tillage Agroecosystems along Two Climatic

Gradients." *Soil Biology and Biochemistry* 31(4). doi: 10.1016/S0038-0717(98)00161-8.

Gadd, Geoffrey M., and Louise de Rome. 1988. "Biosorption of Copper by Fungal Melanin." *Applied Microbiology and Biotechnology* 29(6):610–17. doi: 10.1007/bf00260993.

Gallois, N., J. Templier, and S. Derenne. 2007. "Pyrolysis-Gas Chromatography–Mass Spectrometry of the 20 Protein Amino Acids in the Presence of TMAH." *Journal of Analytical and Applied Pyrolysis* 80(1):216–30. doi: 10.1016/j.jaap.2007.02.010.

Glaser, Bruno, and Wulf Amelung. 2002. "Determination of 13C Natural Abundance of Amino Acid Enantiomers in Soil: Methodological Considerations and First Results." *Rapid Communications in Mass Spectrometry* 16(9):891–98. doi: 10.1002/rcm.650.

Glaser, Bruno, María-Belén Turrión, and Kassem Alef. 2004. "Amino Sugars and Muramic Acid—Biomarkers for Soil Microbial Community Structure Analysis." *Soil Biology and Biochemistry* 36(3):399–407. doi: 10.1016/j.soilbio.2003.10.013.

Godbold, Douglas L., Marcel R. Hoosbeek, Martin Lukac, M. Francesca Cotrufo, Ivan A. Janssens, Reinhart Ceulemans, Andrea Polle, Eef J. Velthorst, Giuseppe Scarascia-Mugnozza, Paolo De Angelis, Franco Miglietta, and Alessandro Peressotti. 2006. "Mycorrhizal Hyphal Turnover as a Dominant Process for Carbon Input into Soil Organic Matter." *Plant and Soil* 281(1–2):15–24. doi: 10.1007/s11104-005-3701-6.

Gooday, Graham W. 1990. "The Ecology of Chitin Degradation." Pp. 387–430 in *Advances in Microbial Ecology*, edited by K. C. Marshall. Springer.

Guggenberger, Georg, Serita D. Frey, Johan Six, Keith Paustian, and Edward T. Elliott.

1999. “Bacterial and Fungal Cell-Wall Residues in Conventional and No-Tillage Agroecosystems.” *Soil Science Society of America Journal* 63(5):1188. doi: 10.2136/sssaj1999.6351188x.

Guignard, C., L. Lemée, and A. Amblès. 2005. “Lipid Constituents of Peat Humic Acids and Humin. Distinction from Directly Extractable Bitumen Components Using TMAH and TEAAc Thermochemolysis.” *Organic Geochemistry* 36(2):287–97. doi: 10.1016/j.orggeochem.2004.07.016.

Harmon, Mark E., Whendee L. Silver, Becky Fasth, Hua Chen, Ingrid C. Burke, William J. Parton, Stephen C. Hart, William S. Currie, and Lidet. 2009. “Long-term Patterns of Mass Loss during the Decomposition of Leaf and Fine Root Litter: An Intersite Comparison.” *Global Change BIology* 15(5):13201338.

Hatcher, Patrick G., Mark A. Nanny, Robert D. Minard, Scott D. Dible, and Daniel M. Carson. 1995. “Comparison of Two Thermochemolytic Methods for the Analysis of Lignin in Decomposing Gymnosperm Wood: The CuO Oxidation Method and the Method of Thermochemolysis with Tetramethylammonium Hydroxide (TMAH).” *Organic Geochemistry* 23(10):881–88. doi: 10.1016/0146-6380(95)00087-9.

Hedges, J. I., G. Eglinton, P. G. Hatcher, D. L. Kirchman, C. Arnosti, S. Derenne, R. P. Evershed, I. Kögel-Knabner, J. W. de Leeuw, R. Littke, W. Michaelis, and J. Rullkötter. 2000. “The Molecularly-Uncharacterized Component of Nonliving Organic Matter in Natural Environments.” *Organic Geochemistry* 31(10):945–58. doi: https://doi.org/10.1016/S0146-6380(00)00096-6.

Helgason, Bobbi L., Fran L. Walley, and James J. Germida. 2009. “Fungal and Bacterial

Abundance in Long-Term No-Till and Intensive-Till Soils of the Northern Great Plains." *Soil Science Society of America Journal* 73(1). doi: 10.2136/sssaj2007.0392.

Hu, S., D. C. Coleman, M. H. Beare, and P. F. Hendrix. 1995. "Soil Carbohydrates in Aggrading and Degrading Agroecosystems: Influences of Fungi and Aggregates." *Agriculture, Ecosystems & Environment* 54(1–2):77–88. doi: 10.1016/0167-8809(95)00588-j.

Hurst, H. M., and G. H. Wagner. 1969. "Decomposition of 14C-Labeled Cell Wall and Cytoplasmic Fractions from Hyaline and Melanic Fungi." *Soil Science Society of America Journal* 33(5):707. doi: 10.2136/sssaj1969.03615995003300050025x.

IPCC. 2013. *Climate Change 2013: The Physical Science Basis*. Contribution of Working Group I to the Fourth Assessment Report of the Intergovernmental Panel on Climate Change.

Jenkinson, D. S., S. P. S. Andrew, J. M. Lynch, M. J. Goss, and P. B. Tinker. 1990. "The Turnover of Organic Carbon and Nitrogen in Soil." *Philosophical Transactions of the Royal Society B: Biological Sciences* 329(1255):361–68. doi: 10.1098/rstb.1990.0177.

Joergensen, R., and F. Wichern. 2008. "Quantitative Assessment of the Fungal Contribution to Microbial Tissue in Soil." *Soil Biology and Biochemistry* 40(12):2977–91. doi: 10.1016/j.soilbio.2008.08.017.

Joffre, R., D. Gillon, P. Dardenne, R. Agneessens, and R. Biston. 1992. "The Use of Near-Infrared Reflectance Spectroscopy in Litter Decomposition Studies." *Annales*

Des Sciences Forestières 49(5):481–88. doi: 10.1051/forest:19920504.

Kallenbach, Cynthia M., Serita D. Frey, and A. Stuart Grandy. 2016. "Direct Evidence for Microbial-Derived Soil Organic Matter Formation and Its Ecophysiological Controls." *Nature Communications* 7:13630.

Kang, Seunghun, and Baoshan Xing. 2005. "Phenanthrene Sorption to Sequentially Extracted Soil Humic Acids and Humins." *Environmental Science & Technology* 39(1):134–40. doi: 10.1021/es0490828.

Klamer, Morten, Michael S. Roberts, Lanfang H. Levine, Bert G. Drake, and Jay L. Garland. 2002. "Influence of Elevated CO2 on the Fungal Community in a Coastal Scrub Oak Forest Soil Investigated with Terminal-Restriction Fragment Length Polymorphism Analysis." *Applied and Environmental Microbiology* 68(9). doi: 10.1128/AEM.68.9.4370-4376.2002.

Klis, Frans M., Pieternella Mol, Klaas Hellingwerf, and Stanley Brul. 2002. "Dynamics of Cell Wall Structure in Saccharomyces Cerevisiae." *FEMS Microbiology Reviews* 26(3):239–56. doi: 10.1111/j.1574-6976.2002.tb00613.x.

Kogej, Tina, Anna A. Gorbushina, and Nina Gunde-Cimerman. 2006. "Hypersaline Conditions Induce Changes in Cell-Wall Melanization and Colony Structure in a Halophilic and a Xerophilic Black Yeast Species of the Genus Trimmatostroma." *Mycological Research* 110(6):713–24. doi: 10.1016/j.mycres.2006.01.014.

Kögel-Knabner, I. 2002. "The Macromolecular Organic Composition of Plant and Microbial Residues as Inputs to Soil Organic Matter." *Soil Biology and Biochemistry* 34(2):139–62. doi: 10.1016/s0038-0717(01)00158-4.

Kögel-Knabner, Ingrid. 2000. “Analytical Approaches for Characterizing Soil Organic Matter.” *Organic Geochemistry* 31(7–8):609–25. doi: 10.1016/s0146-6380(00)00042-5.

Koide, Roger T., and Glenna M. Malcolm. 2009. “N Concentration Controls Decomposition Rates of Different Strains of Ectomycorrhizal Fungi.” *Fungal Ecology* 2(4):197–202. doi: 10.1016/j.funeco.2009.06.001.

Kollár, Roman, Bruce B. Reinhold, Eva Petráková, Herman J. C. Yeh, Gilbert Ashwell, Jana Drgonová, Johan C. Kapteyn, Frans M. Klis, and Enrico Cabib. 1997. “Architecture of the Yeast Cell Wall.” *Journal of Biological Chemistry* 272(28):17762–75. doi: 10.1074/jbc.272.28.17762.

Langley, J. Adam, and Bruce A. Hungate. 2003. “Mycorrhizal Controls on Belowground Litter Quality.” *Ecology* 84(9):2302–12. doi: 10.1890/02-0282.

Latgé, Jean-Paul. 2007. “The Cell Wall: A Carbohydrate Armour for the Fungal Cell.” *Molecular Microbiology* 66(2):279–90. doi: 10.1111/j.1365-2958.2007.05872.x.

Leal, Juan Antonio, Alicia Prieto, Manuel Bernabé, and David L. Hawksworth. 2010. “An Assessment of Fungal Wall Heteromannans as a Phylogenetically Informative Character in Ascomycetes.” *FEMS Microbiology Reviews* 34(6):986–1014. doi: 10.1111/j.1574-6976.2010.00225.x.

Lehmann, Johannes, and Markus Kleber. 2015. “The Contentious Nature of Soil Organic Matter.” *Nature* 528:60.

Lehtonen, T., J. Peuravuori, and K. Pihlaja. 2003. “Comparison of Quaternary Methyl-, Ethyl- and Butylammonium Hydroxides as Alkylating Reagents in Pyrolysis-

GC/MS Studies of Aquatic Fulvic Acid." *Journal of Analytical and Applied Pyrolysis* 68–69:315–29. doi: 10.1016/s0165-2370(03)00050-0.

Liang, Chao, Guang Cheng, Devin L. Wixon, and Teri C. Balser. 2010. "An Absorbing Markov Chain Approach to Understanding the Microbial Role in Soil Carbon Stabilization." *Biogeochemistry* 106(3):303–9. doi: 10.1007/s10533-010-9525-3.

Linhares, L. F., and J. P. Martin. 1978. "Decomposition in Soil of the Humic Acid-Type Polymers (Melanins) of Eurotium Echinulatum, Aspergillus Glaucus Sp. and Other Fungi." *Soil Science Society of America Journal* 42(5):738. doi: 10.2136/sssaj1978.03615995004200050016x.

Lloyd, J., and J. A. Taylor. 1994. "On the Temperature Dependence of Soil Respiration." *Functional Ecology* 8(3):315. doi: 10.2307/2389824.

Maillard, François, Jonathan Schilling, Erin Andrews, Kathryn M. Schreiner, and Peter Kennedy. 2020. "Functional Convergence in the Decomposition of Fungal Necromass in Soil and Wood." *FEMS Microbiology Ecology* 96(2). doi: 10.1093/femsec/fiz209.

Malik, K. A., and K. Haider. 1982. "Decomposition of 14C-Labelled Melanoid Fungal Residues in a Marginally Sodic Soil." *Soil Biology and Biochemistry* 14(5):457–60. doi: 10.1016/0038-0717(82)90104-3.

Manzoni, Stefano, and Amilcare Porporato. 2009. "Soil Carbon and Nitrogen Mineralization: Theory and Models across Scales." *Soil Biology and Biochemistry* 41(7):1355–79. doi: https://doi.org/10.1016/j.soilbio.2009.02.031.

Marshall, Carolyn B., Jennie R. McLaren, and Roy Turkington. 2011. "Soil Microbial

Communities Resistant to Changes in Plant Functional Group Composition." *Soil Biology and Biochemistry* 43(1). doi: 10.1016/j.soilbio.2010.09.016.

Miltner, Anja, Petra Bombach, Burkhard Schmidt-Brücken, and Matthias Kästner. 2011. "SOM Genesis: Microbial Biomass as a Significant Source." *Biogeochemistry* 111(1–3):41–55. doi: 10.1007/s10533-011-9658-z.

Miltner, Anja, Reimo Kindler, Heike Knicker, Hans-Hermann Richnow, and Matthias Kästner. 2009. "Fate of Microbial Biomass-Derived Amino Acids in Soil and Their Contribution to Soil Organic Matter." *Organic Geochemistry* 40(9):978–85. doi: https://doi.org/10.1016/j.orggeochem.2009.06.008.

Moore, David, Geoffrey Robson, and Anthony Trinci. 2011. *21st Century Guidebook to Fungi*. Cambridge University Press.

Moore, John C., Eric L. Berlow, David C. Coleman, Peter C. De Suiter, Quan Dong, Alan Hastings, Nancy Collins Johnson, Kevin S. McCann, Kim Melville, Peter J. Morin, Knute Nadelhoffer, Amy D. Rosemond, David M. Post, John L. Sabo, Kate M. Scow, Michael J. Vanni, and Diana H. Wall. 2004. "Detritus, Trophic Dynamics and Biodiversity." *Ecology Letters* 7(7).

Morais, Tiago G., Ricardo F. M. Teixeira, and Tiago Domingos. 2019. "Detailed Global Modelling of Soil Organic Carbon in Cropland, Grassland and Forest Soils." *PLoS ONE* 14(9). doi: 10.1371/journal.pone.0222604.

Nishimura, Mitsugu, and Tadashiro Koyama. 1977. "The Occurrence of Stanols in Various Living Organisms and the Behavior of Sterols in Contemporary Sediments." *Geochimica et Cosmochimica Acta* 41(3):379–85. doi: 10.1016/0016-

7037(77)90265-4.

Nosanchuk, Joshua D., Ruth E. Stark, and Arturo Casadevall. 2015. “Fungal Melanin: What Do We Know About Structure?” *Frontiers in Microbiology* 6. doi: 10.3389/fmicb.2015.01463.

Nylund, J., and H. Wallander. 1992. “Ergosterol Analysis as a Means of Quantifying Mycorrhizal Biomass.” *Methods in Microbiology* 24.

Olson, Jerry S. 1963. “Energy Storage and the Balance of Producers and Decomposers in Ecological Systems.” *Ecology* 44(2):322–31. doi: 10.2307/1932179.

Parton, W. J., J. M. O. Scurlock, D. S. Ojima, T. G. Gilmanov, R. J. Scholes, D. S. Schimel, T. Kirchner, J. C. Menaut, T. Seastedt, E. Garcia Moya, Apinan Kamnalrut, and J. I. Kinyamario. 1993. “Observations and Modeling of Biomass and Soil Organic Matter Dynamics for the Grassland Biome Worldwide.” *Global Biogeochemical Cycles* 7(4):785–809. doi: 10.1029/93gb02042.

Parton, William J., Melannie Hartman, Dennis Ojima, and David Schimel. 1998. “DAYCENT and Its Land Surface Submodel: Description and Testing.” *Global and Planetary Change* 19(1–4):35–48. doi: 10.1016/s0921-8181(98)00040-x.

Pasanen, A., K. Yli-Pietil, P. Pasanen, P. Kalliokoski, and J. Tarhanen. 1999. “Ergosterol Content in Various Fungal Species and Biocontaminated Building Materials.” *Applied and Environmental Microbiology* 65(1):138–42.

Paul, Eldor A., Ronald F. Follett, Michelle Haddix, and Elizabeth Pruessner. 2011. “Soil N Dynamics Related to Soil C and Microbial Changes During Long-Term Incubation.” *Soil Science* 176(10):527–36. doi: 10.1097/ss.0b013e31822ce6e8.

Phillips, Rebecca L., Donald R. Zak, William E. Holmes, and David C. White. 2002. "Microbial Community Composition and Function beneath Temperate Trees Exposed to Elevated Atmospheric Carbon Dioxide and Ozone." *Oecologia* 131(2). doi: 10.1007/s00442-002-0868-x.

Piccolo, Alessandro, Pellegrino Conte, Enrico Trivellone, Barend van Lagen, and Peter Buurman. 2002. "Reduced Heterogeneity of a Lignite Humic Acid by Preparative HPSEC Following Interaction with an Organic Acid. Characterization of Size-Separates by Pyr-GC-MS And 1H-NMR Spectroscopy." *Environmental Science & Technology* 36(1):76–84. doi: 10.1021/es010981v.

Prewitt, Lynn, Youngmin Kang, Madhavi L. Kakumanu, and Mark Williams. 2014. "Fungal and Bacterial Community Succession Differs for Three Wood Types during Decay in a Forest Soil." *Microbial Ecology* 68(2). doi: 10.1007/s00248-014-0396-3.

Rillig, Matthias C., B. F. Christopher, and Michael F. Allen. 1999. "Fungal Root Colonization Responses in Natural Grasslands after Long-Term Expousre to Elevated Atmospheric CO2." *Global Change Biology* 5(5). doi: 10.1046/j.1365-2486.1999.00251.x.

Roberts, P., and D. L. Jones. 2012. "Microbial and Plant Uptake of Free Amino Sugars in Grassland Soils." *Soil Biology and Biochemistry* 49:139–49. doi: 10.1016/j.soilbio.2012.02.014.

Ryan, Maeve E. 2019. "Factors Controlling the Decomposition of Ectomycorrhizal Fungal Tissue and the Formation of Soil Organic Matter." University of Minnesota.

Ryan, Maeve E., Kathryn M. Schreiner, Jenna T. Swenson, Joseph Gagne, and Peter G.

Kennedy. 2020. “Rapid Changes in the Chemical Composition of Degrading Ectomycorrhizal Fungal Necromass.” *Fungal Ecology* 45. doi: 10.1016/j.funeco.2020.100922.

Schmidt, Michael W. I., Margaret S. Torn, Samuel Abiven, Thorsten Dittmar, Georg Guggenberger, Ivan A. Janssens, Markus Kleber, Ingrid Kögel-Knabner, Johannes Lehmann, David A. C. Manning, Paolo Nannipieri, Daniel P. Rasse, Steve Weiner, and Susan E. Trumbore. 2011. “Persistence of Soil Organic Matter as an Ecosystem Property.” *Nature* 478(7367):49–56. doi: 10.1038/nature10386.

Schreiner, Kathryn M., Neal E. Blair, and Louise M. Levinson, William Egerton-Warburton. 2014. “Contribution of Fungal Macromolecules to Soil Carbon Sequestration.” Pp. 155–61 in *Soil Carbon*, edited by A. Hartemink and K. McSweeney. Springer.

Schulten, H., and C. Sorge. 1995. “Pyrolysis Methylation—Mass Spectrometry of Whole Soils.” *European Journal of Soil Science* 46(4):567–79. doi: 10.1111/j.1365-2389.1995.tb01353.x.

Schwarzinger, Clemens. 2005. “Identification of Fungi with Analytical Pyrolysis and Thermally Assisted Hydrolysis and Methylation.” *Journal of Analytical and Applied Pyrolysis* 74(1–2):26–32. doi: 10.1016/j.jaap.2004.11.025.

Shadkami, Farzad, and Robert Helleur. 2010. “Recent Applications in Analytical Thermochemolysis.” *Journal of Analytical and Applied Pyrolysis* 89(1):2–16. doi: 10.1016/j.jaap.2010.05.007.

Simpson, André J., Myrna J. Simpson, Emma Smith, and Brian P. Kelleher. 2007.

"Microbially Derived Inputs to Soil Organic Matter: Are Current Estimates Too Low?" *Environmental Science & Technology* 41(23):8070–76. doi: 10.1021/es071217x.

Simpson, Myrna J., and André J. Simpson. 2012. "The Chemical Ecology of Soil Organic Matter Molecular Constituents." *Journal of Chemical Ecology* 38(6):768–84. doi: 10.1007/s10886-012-0122-x.

Singaravelan, Natarajan, Isabella Grishkan, Alex Beharav, Kazumasa Wakamatsu, Shosuke Ito, and Eviatar Nevo. 2008. "Adaptive Melanin Response of the Soil Fungus Aspergillus Niger to UV Radiation Stress at 'Evolution Canyon', Mount Carmel, Israel." *PLoS ONE* 3(8):e2993. doi: 10.1371/journal.pone.0002993.

Six, J., R. Conant, E. Paul, and K. Paustian. 2002. "Stabilization Mechanisms of Soil Organic Matter: Implications for C-Saturation of Soils." *Plant and Soil* 241(2):155–76.

Six, J., S. D. Frey, R. K. Thiet, and K. M. Batten. 2006. "Bacterial and Fungal Contributions to Carbon Sequestration in Agroecosystems." *Soil Science Society of America Journal* 70(2):555. doi: 10.2136/sssaj2004.0347.

Skjemstad, J. O., L. R. Spouncer, B. Cowie, and R. S. Swift. 2004. "Calibration of the Rothamsted Organic Carbon Turnover Model (RothC Ver. 26.3), Using Measurable Soil Organic Carbon Pools." *Australian Journal of Soil Research* 42(1):79. doi: 10.1071/sr03013.

Sobeih, Karina L., Mark Baron, and Jose Gonzalez-Rodriguez. 2008. "Recent Trends and Developments in Pyrolysis–Gas Chromatography." *Journal of Chromatography A*

1186(1–2):51–66. doi: 10.1016/j.chroma.2007.10.017.

Spence, Adrian, Andre J. Simpson, David J. Mcnally, Brian W. Moran, Margaret V McCaul, Kris Hart, Brett Paull, and Brian P. Kelleher. 2011. "The Degradation Characteristics of Microbial Biomass in Soil." *Geochimica et Cosmochimica Acta* 75(10):2571–81. doi: 10.1016/j.gca.2011.03.012.

Steinberg, Spencer M., Elkas L. Nemr, and Mark Rudin. 2008. "Characterization of the Lignin Signature in Lake Mead, NV, Sediment: Comparison of on-Line Flash Chemopyrolysis (600°C) and off-Line Chemolysis (250°C)." *Environmental Geochemistry and Health* 31(3):339–52. doi: 10.1007/s10653-008-9174-9.

Stevenson, F. J. 1983. "Isolation and Identification of Amino Sugars in Soil." *Soil Science Society of America Journal* 47(1):61. doi: 10.2136/sssaj1983.03615995004700010012x.

Strickland, Michael S., and Johannes Rousk. 2010. "Considering Fungal: Bacterial Dominance in Soils - Methods, Controls, and Ecosystem Implications." *Soil Biology and Biochemistry* 42(9).

Sutton, Rebecca, and Garrison Sposito. 2005. "Molecular Structure in Soil Humic Substances: The New View." *Environmental Science & Technology* 39(23):9009–15. doi: 10.1021/es050778q.

Taub, D. 2010. "Effects of Rising Atmospheric Concentrations of Carbon Dioxide on Plants." *Nature Education Knowledge* 1(8).

Taylor, Barry R., Dennis Parkinson, and William F. J. Parsons. 1989. "Nitrogen and Lignin Content as Predictors of Litter Decay Rates: A Microcosm Test." *Ecology*

70(1):97–104. doi: 10.2307/1938416.

Tietema, A., and W. W. Wessel. 1994. “Microbial Activity and Leaching during Initial Oak Leaf Litter Decomposition.” *Biology and Fertility of Soils* 18(1). doi: 10.1007/BF00336444.

Tisdall, J. M., and J. M. Oades. 1982. “Organic Matter and Water-Stable Aggregates in Soils.” *Journal of Soil Science* 33(2):141–63. doi: 10.1111/j.1365-2389.1982.tb01755.x.

Todd-Brown, K. E. O., J. T. Randerson, W. M. Post, F. M. Hoffman, C. Tarnocai, E. A. G. Schuur, and S. D. Allison. 2013. “Causes of Variation in Soil Carbon Simulations from CMIP5 Earth System Models and Comparison with Observations.” *Biogeosciences* 10(3):1717–36. doi: 10.5194/bg-10-1717-2013.

Treseder, K. K., and M. F. Allen. 2000. “Mycorrhizal Fungi Have a Potential Role in Soil Carbon Storage under Elevated CO2 and Nitrogen Deposition.” *New Phytologist* 147(1):189–200. doi: 10.1046/j.1469-8137.2000.00690.x.

Tsai, Cheng-Sheng, Ken Killham, and Malcolm S. Cresser. 1997. “Dynamic Response of Microbial Biomass, Respiration Rate and ATP to Glucose Additions.” *Soil Biology and Biochemistry* 29(8):1249–56. doi: 10.1016/s0038-0717(97)00020-5.

Verma, L., J. P. Martin, and K. Haider. 1975. “Decomposition of Carbon-14 Labeled Proteins, Peptides, and Amino Acids; Free and Complexed with Humic Polymers.” *Soil Science Society of America Journal* 39(2):279. doi: 10.2136/sssaj1975.03615995003900020018x.

Waldrop, M. P., and M. K. Firestone. 2004. “Altered Utilization Patterns of Young and

Old Soil C by Microorganisms Caused by Temperature Shifts and N Additions." *Biogeochemistry* 67(2). doi: 10.1023/B:BIOG.0000015321.51462.41.

Wang, Yulin, Philip Aisen, and Arturo Casadevall. 1995. "Cryptococcus Neoformans Melanin and Virulence: Mechanism of Action." *Infection and Immunity* 63(8):3131–36.

Watson, Jonathan S., Mark A. Sephton, Sarah V Sephton, Stephen Self, Wesley T. Fraser, Barry H. Lomax, Iain Gilmour, Charles H. Wellman, and David J. Beerling. 2007. "Rapid Determination of Spore Chemistry Using Thermochemolysis Gas Chromatography-Mass Spectrometry and Micro-Fourier Transform Infrared Spectroscopy." *Photochemical & Photobiological Sciences* 6(6):689. doi: 10.1039/b617794h.

Webster, E. A., J. A. Chudek, and D. W. Hopkins. 1997. "Fates of 13 C from Enriched Glucose and Glycine in an Organic Soil Determined by Solid-State NMR." *Biology and Fertility of Soils* 25(4):389–95. doi: 10.1007/s003740050330.

Webster, J. R., and E. F. Benfield. 1986. "Vascular Plant Breakdown in Freshwater Ecosystems." *Annual Review of Ecology and Systematics. Vol. 17*. doi: 10.1146/annurev.es.17.110186.003031.

Westrich, Joseph T., and Robert A. Berner. 1984. "The Role of Sedimentary Organic Matter in Bacterial Sulfate Reduction: TheGmodel Tested1." *Limnology and Oceanography* 29(2):236–49. doi: 10.4319/lo.1984.29.2.0236.

Wilkinson, Anna, Ian J. Alexander, and David Johnson. 2011. "Species Richness of Ectomycorrhizal Hyphal Necromass Increases Soil CO2 Efflux under Laboratory

Conditions." *Soil Biology and Biochemistry* 43(6):1350–55. doi: 10.1016/j.soilbio.2011.03.009.

Xiong, Li, Xiaoyu Liu, Giovanni Vinci, Riccardo Spaccini, Marios Drosos, Lianqing Li, Alessandro Piccolo, and Genxing Pan. 2019. "Molecular Changes of Soil Organic Matter Induced by Root Exudates in a Rice Paddy under CO2 Enrichment and Warming of Canopy Air." *Soil Biology and Biochemistry* 137. doi: 10.1016/j.soilbio.2019.107544.

Xu, Ming, Franco Basile, and Kent J. Voorhees. 2000. "Differentiation and Classification of User-Specified Bacterial Groups by in Situ Thermal Hydrolysis and Methylation of Whole Bacterial Cells with Tert-Butyl Bromide Chemical Ionization Ion Trap Mass Spectrometry." *Analytica Chimica Acta* 418(2):119–28. doi: 10.1016/s0003-2670(00)00952-1.

Zeglin, Lydia H., Laurel A. Kluber, and David D. Myrold. 2012. "The Importance of Amino Sugar Turnover to C and N Cycling in Organic Horizons of Old-Growth Douglas-Fir Forest Soils Colonized by Ectomycorrhizal Mats." *Biogeochemistry* 112(1–3):679–93. doi: 10.1007/s10533-012-9746-8.

Zhang, X., J. Brown, J. van Heemst, A. Palumbo, and P. Hatcher. 2001. "Characterization of Amino Acids and Proteinaceous Materials Using Online Tetramethylammonium Hydroxide (TMAH) Thermochemolysis and Gas Chromatography-Mass Spectrometry Technique." *Journal of Analytical and Applied Pyrolysis* 61:181–93.

Zhong, Junyan, Susana Frases, Hsin Wang, Arturo Casadevall, and Ruth E. Stark. 2008.

"Following Fungal Melanin Biosynthesis with Solid-State NMR: Biopolymer Molecular Structures and Possible Connections to Cell-Wall Polysaccharides†." *Biochemistry* 47(16):4701–10. doi: 10.1021/bi702093r.

Zimmermann, M., J. Leifeld, M. W. I. Schmidt, P. Smith, and J. Fuhrer. 2007. "Measured Soil Organic Matter Fractions Can Be Related to Pools in the RothC Model." *European Journal of Soil Science* 58(3):658–67. doi: 10.1111/j.1365-2389.2006.00855.x.